

1 **Detecting context-dependence in the expression of life history tradeoffs**

2

3 Louis Bliard ^{1*}, Jordan S. Martin ^{2*}, Maria Paniw ^{1,3}, Daniel T. Blumstein ^{4,5}, Julien G.A. Martin ⁶,
4 Josephine M. Pemberton ⁷, Daniel H. Nussey ⁷, Dylan Z. Childs ⁸, Arpat Ozgul ¹

5

6 1 Department of Evolutionary Biology and Environmental Studies, Zurich University, Zurich,
7 Switzerland

8 2 Institute of Evolutionary Medicine, Zurich University, Zurich, Switzerland

9 3 Department of Conservation Biology, Estación Biológica de Doñana (EBD-CSIC), Seville, Spain

10 4 Department of Ecology and Evolutionary Biology, University of California Los Angeles, Los
11 Angeles, California, USA

12 5 The Rocky Mountain Biological Laboratory, Crested Butte, Colorado, USA

13 6 Department of Biology, University of Ottawa, Ottawa, Ontario, Canada

14 7 Institute of Ecology and Evolution, University of Edinburgh, Edinburgh, UK

15 8 Department of Animal and Plant Sciences, University of Sheffield, Sheffield, UK

16

17 * Shared first authorship

18

19 Corresponding author: bliard.louis@gmail.com / louis.bliard@uzh.ch

20

21

22

23
24
25
26
27
28
29
30
31
32
33
34
35
36
37
38
39
40
41
42
43

Abstract

Life history tradeoffs are one of the central tenets of evolutionary demography. Tradeoffs, depicting negative covariances between individuals' life history traits, can arise from genetic constraints, or from a finite amount of resources that each individual has to allocate in a zero-sum game between somatic and reproductive functions. While theory predicts that tradeoffs are ubiquitous, empirical studies have often failed to detect such negative covariances in wild populations. One way to improve the detection of tradeoffs is by accounting for the environmental context, as tradeoff expression may depend on environmental conditions. However, current methodologies usually search for fixed covariances between traits, thereby ignoring their context dependence. Here, we present a hierarchical multivariate 'covariance reaction norm' model, adapted from Martin (2023), to help detect context dependence in the expression of life-history tradeoffs using demographic data. The method allows continuous variation in the phenotypic correlation between traits. We validate the model on simulated data for both intraindividual and intergenerational tradeoffs. We then apply it to empirical datasets of yellow-bellied marmots (*Marmota flaviventer*) and Soay sheep (*Ovis aries*) as a proof-of-concept showing that new insights can be gained by applying our methodology, such as detecting tradeoffs only in specific environments. We discuss its potential for application to many of the existing long-term demographic datasets and how it could improve our understanding of tradeoff expression in particular, and life history theory in general.

Introduction

44 Demographic tradeoffs, which are characterized as negative covariances between fitness
45 components such as somatic or reproductive traits, are central to life history theory (Stearns,
46 1989), and are thought to constrain and organize much of the life history diversity that exists
47 (Bielby et al., 2007; Healy et al., 2019; Salguero-Gómez et al., 2016; Stearns, 1984). They originate
48 from the basic fact that the total amount of resources or energy acquired by any one individual
49 is limited, and has to be shared among several of the individual's fitness-related traits. In such a
50 zero-sum game and in the absence of change in the total amount of resources acquired, any
51 increase in the allocation of resources towards a specific fitness component will have to be at the
52 expense of another fitness component. While tradeoffs stem from individual processes, these
53 covariances can scale up to different levels of organization (Agrawal, 2020; Bliard et al., 2024). If
54 tradeoffs did not exist, selection would maximize all fitness-related traits simultaneously and
55 would lead to the impossible "darwinian demons" (Law, 1979). Therefore, tradeoffs should be
56 faced by all organisms and are, in theory, ubiquitous (Stearns, 1989, 1992; Williams, 1966). They
57 can come in several forms (Stearns, 1989), being either intraindividual (traits involved relate to
58 the fitness of the same individual) or intergenerational (traits involved relate to the fitness of a
59 parent-offspring pair; e.g., offspring quantity-quality tradeoff). Despite their expected
60 universality and being sought-after by evolutionary ecologists and biodemographers alike, life-
61 history tradeoffs have been surprisingly hard to detect in wild populations (Chang et al., 2023;
62 Metcalf, 2016; van Noordwijk & de Jong, 1986), with successful probes too often confined to
63 experimental approaches.

64 Several reasons could explain why tradeoffs are hard to detect in wild populations. First,
65 we often expect traits to covary in a simple bivariate manner following the Y-model of resource

66 allocation, where any resources diverted from a trait will be allocated to the other one (de Jong
67 & van Noordwijk, 1992). Thus while we are often analyzing a single pair of traits at a time, tradeoff
68 structures are often more complex. For instance, many more than two traits are likely to be
69 involved in the resource allocation process (Cressler et al., 2017; de Jong, 1993; Pease & Bull,
70 1988), sometimes leading to complex hierarchical allocation trees, potentially resulting in some
71 pairs of traits not covarying negatively (Gascoigne et al., 2022). Second, life history traits can
72 covary at different levels. While tradeoffs result from individuals' resource allocation processes,
73 biodemographers often study tradeoffs as the temporal correlations among demographic rates
74 at the population level (Compagnoni et al., 2016; Fay et al., 2020; Fay, Hamel, et al., 2022; van
75 Tienderen, 1995). Tradeoffs can occasionally scale up to cause negative temporal covariances at
76 the population level (van Tienderen, 1995), but in most cases these covariances are the results
77 of environmental stochasticity and demographic reaction norms to shared ecological drivers (Fay,
78 Hamel, et al., 2022; Knops et al., 2007; Paniw et al., 2020). Third, even though tradeoffs might be
79 present, individual heterogeneity can mask their presence among individuals. This specific
80 ecological version of Simpson's paradox (Simpson, 1951) has been demonstrated by van
81 Noordwijk and de Jong (1986): when the among-individual variance in resource acquisition is
82 greater than the among-individual variance in resource allocation, the tradeoff is not expressed
83 among individuals — even though it is theoretically present within individuals. In addition,
84 expression of a tradeoff among individuals can also be influenced if the allocation and acquisition
85 processes are not independent (Descamps et al., 2016; Fischer et al., 2009; Robinson &
86 Beckerman, 2013). Altogether, this makes the detection of tradeoffs in wild populations difficult.

87 How much individuals vary in acquisition and allocation of resources determines if a
88 tradeoff is detected among individuals (Metcalf, 2016; Reznick et al., 2000; van Noordwijk & de
89 Jong, 1986). Part of this variance might be fixed, stemming from genetic, developmental, or
90 consistent behavioral differences that constrain how much resources are acquired and allocated
91 to somatic vs. reproductive functions (Réale et al., 2007; Wilson & Nussey, 2010). The remaining
92 variance is likely to be plastic (Spigler & Woodard, 2019), where acquisition vs. allocation likely
93 depends on the environmental context (Cohen et al., 2020; Sgrò & Hoffmann, 2004; Stearns et
94 al., 1991). For instance, in several species, no tradeoffs were found among captive animals fed
95 *ad libitum* (Kengeri et al., 2013; Landes et al., 2019; Ricklefs & Cadena, 2007). Similarly, controlled
96 laboratory experiments on several species have shown that tradeoffs detection and strength
97 were dependent on resource abundance (Gebhardt & Stearns, 1988; Messina & Fry, 2003;
98 Messina & Slade, 1999; Spigler & Woodard, 2019). However, despite evidence that tradeoff
99 expression depends on the environmental context, statistical methods to detect this context
100 dependence in wild populations have, to date, rarely been applied.

101 Multivariate models are commonly employed to detect tradeoffs in wild populations
102 (Cam et al. 2002, 2013; Hamel et al. 2018; Paterson et al. 2018; Fay et al. 2022a). In quantitative
103 genetics, such models allow for the simultaneous analysis of multiple dependent variables like
104 fecundity, growth, and survival (Kruuk et al. 2008; Wilson et al. 2010). These variables each have
105 their own predictors, and the models estimate the correlated residual variances unaccounted for
106 by the primary predictors. These models can be used to study residual correlations between traits
107 at different levels, such as among-year correlation and among-individual correlation. For
108 example, after accounting for primary predictors, such models quantify whether years with high

109 survival in a population are also years with high recruitment; or whether individuals with higher
110 fecundity have lower or higher growth rates. However, these correlations among residual
111 variances are estimated as fixed. Estimating fixed correlations might not necessarily be
112 problematic in the case of experimental work, in which environmental conditions can be held
113 constant within each treatment. However, wild populations are unlikely to experience fixed
114 conditions, as the environmental context will vary in a continuous fashion, hence influencing the
115 expression of tradeoffs. Therefore, there is a need to analyse and predict continuous variation of
116 phenotypic correlations.

117 Here, we repurpose a hierarchical multivariate ‘covariance reaction norm’ (hereafter
118 CRN) model recently developed by Martin (2023), which allows the incorporation of continuous
119 predictors directly on the covariance matrix, for application to sampling designs typical in
120 population ecology, enabling the study of the context-dependent expression of tradeoffs. As a
121 proof-of-concept, we first validate this model on two simulated datasets, respectively focusing
122 on an intergenerational tradeoff and an intraindividual tradeoff. We then apply our model on
123 two empirical datasets of wild populations of yellow-bellied marmots *Marmota flaviventer* and
124 Soay sheep *Ovis aries*. Prior studies have explored tradeoffs between vital rates in both species
125 (Kroeger et al., 2020; Tavecchia et al., 2005). For instance, in yellow-bellied marmots, a quality-
126 quantity tradeoff in offspring has been observed for older mothers. In Soay sheep, the costs of
127 reproduction have been particularly evident for breeding ewes in high-density populations or
128 following harsh winters. However, the environmental context-dependence of these tradeoffs has
129 yet to be studied explicitly. In the marmots, which inhabit high-altitude, highly seasonal
130 environments, and the sheep, which face severe winter storms and fluctuating population

131 densities, we hypothesize that tradeoffs are more likely to manifest under unfavorable ecological
132 conditions (Cohen et al., 2020; Sgrò & Hoffmann, 2004).

133 **Methods**

134 The model

135 In this study, we employ a newly introduced CRN model (Martin, 2023), which has been
136 developed as a quantitative genetic model to predict continuous changes in trait associations
137 when either genetic data or repeated individual measurements are available for all phenotypes
138 of interest. A key assumption of multivariate models thus far has been that phenotypic
139 correlations caused by tradeoffs are fixed through time or space (Cam et al., 2002; Hamel et al.,
140 2018). The CRN approach provides a solution to this general challenge, by allowing for phenotypic
141 covariances to vary in response to variation in the environment, for example, estimating under
142 which conditions among-individual variance in resources allocation is larger than among-
143 individual variance in acquisition (van Noordwijk & de Jong, 1986). In the present study, we
144 extend application of this general CRN approach to the detection of context-dependent tradeoffs
145 (here defined as among-individual correlations even though both are not always equivalent)
146 between life history traits, with special consideration to sampling conditions typical of long-term
147 field research in population ecology. Specifically, we examine the use of bivariate CRN models to
148 test for the presence of phenotypic tradeoffs when repeated individual measurements are
149 lacking in a given environmental context (e.g., during a specific sampling event such as a breeding
150 season or a year). These are typical situations in field research that motivate further development
151 of the quantitative genetic models proposed by Martin (2023).

152 Before delving into the specifics of the model, note that in all the following models
153 presented, measurements of the same individuals observed in different contexts are considered
154 independent (see supplementary materials Section S1 for more details). This necessary
155 simplification has potential consequences when searching for the phenotypic manifestation of
156 tradeoffs, as fixed heterogeneity across ecological contexts cannot be properly disentangled from
157 context-dependent heterogeneity, which might lead to issues especially in long-lived species that
158 are observed across many different contexts. Nonetheless, this simplification does not impede
159 our ability to detect context-dependence of among-individual correlations (supplementary
160 materials Section S1). Consider a CRN model investigating how environmental contexts C and
161 individual factors affect the phenotypic means of $\beta_{\mu 1}$ and $\beta_{\mu 2}$ and among-individual correlations
162 β_r between two Gaussian life history trait measures \mathbf{z}_1 and \mathbf{z}_2 with repeated individual
163 measurements in each environmental context. \mathbf{X}_1 and \mathbf{X}_2 are $N \times P$ matrices of N measurements
164 of P predictors. We begin by focusing on linear models to simplify notation and aid
165 comprehension, with generalized models for non-Gaussian distributions discussed further below.
166 Following Martin (2023) in the absence of genetic data, our bivariate phenotypic model is given
167 by

$$\begin{aligned}\mathbf{z}_1 &= \mathbf{X}_1 \boldsymbol{\beta}_{\mu 1} + \mathbf{W} \boldsymbol{\alpha}_{1(C)} + \boldsymbol{\epsilon}_{1(C)} \\ \mathbf{z}_2 &= \mathbf{X}_2 \boldsymbol{\beta}_{\mu 2} + \mathbf{W} \boldsymbol{\alpha}_{2(C)} + \boldsymbol{\epsilon}_{2(C)}\end{aligned}\tag{1.1}$$

$$\begin{aligned}[\boldsymbol{\alpha}_{1(C)}, \boldsymbol{\alpha}_{2(C)}] &\sim \mathbf{N}(\mathbf{0}, \mathbf{P}_{(C)}) \\ [\boldsymbol{\epsilon}_1, \boldsymbol{\epsilon}_2] &\sim \mathbf{N}(\mathbf{0}, \boldsymbol{\Sigma}_{(C)})\end{aligned}$$

168

169 Trait values are expressed as a function of the average effects $\beta_{\mu 1}$ and $\beta_{\mu 2}$ of \mathbf{X}_1 and \mathbf{X}_2 on each
170 phenotype, as well as among-individual effects $\alpha_{1(c)}$ and $\alpha_{2(c)}$ that are repeatable across
171 measurements and within-individual effects $\epsilon_{1(c)}$ and $\epsilon_{2(c)}$ that are variable across measurements.
172 The model matrix \mathbf{W} (an $N \times J$ matrix for J subjects) structures the among-individual effects $\alpha_{(c)}$
173 across repeated measurements. (Co)variances between independent among- and within-
174 individual effects are respectively described by \mathbf{P} and $\mathbf{\Sigma}$ covariance matrices. To detect context-
175 dependent tradeoff expression, we use environmental information in \mathbf{X}_3 (an $C \times P$ matrix of C
176 environmental contexts of P predictors) to predict the among-individual trait covariance matrix
177 $\mathbf{P}_{(c)}$.

$$\mathbf{P}_{(c)} = \begin{bmatrix} \sigma_{\alpha_1(c)}^2 & r_{\alpha(c)} \sigma_{\alpha_1(c)} \sigma_{\alpha_2(c)} \\ r_{\alpha(c)} \sigma_{\alpha_2(c)} \sigma_{\alpha_1(c)} & \sigma_{\alpha_2(c)}^2 \end{bmatrix} \quad (1.2)$$

$$\text{atanh}(r_{\alpha(c)}) = \mathbf{X}_3 \boldsymbol{\beta}_r$$

178
179 where the inverse hyperbolic tangent function $\text{atanh}(r) = \text{logit}([r + 1]/2)/2$ is used as a link
180 function to model additive environmental effects $\boldsymbol{\beta}_r$ on the logit scale while retaining the $[-1,1]$
181 scaling of the correlation coefficient r . This is akin to a logistic regression with bounds in $[-1,1]$
182 instead of $[0,1]$. The same approach can be taken to describe changes in within-individual
183 variation across environmental contexts.

$$\mathbf{\Sigma}_{(c)} = \begin{bmatrix} \sigma_{\epsilon_1(c)}^2 & r_{\epsilon(c)} \sigma_{\epsilon_1(c)} \sigma_{\epsilon_2(c)} \\ r_{\epsilon(c)} \sigma_{\epsilon_2(c)} \sigma_{\epsilon_1(c)} & \sigma_{\epsilon_2(c)}^2 \end{bmatrix} \quad (1.3)$$

$$\text{atanh}(r_{\epsilon(c)}) = \mathbf{X}_3 \boldsymbol{\beta}_{r_\epsilon}$$

184
185 Direct prediction of the transformed correlation coefficient is useful because we are
186 principally interested in $r_{(c)}$ as an indicator of putative tradeoffs, rather than the covariance
187 $P_{1,2(c)} = r_{(c)}\sigma_1\sigma_2$ per se. Changes in the scale $\sigma_1\sigma_2$ of life history trait variation may occur

188 independently of changes in positive or negative trait association among individuals, but these
189 effects will be confounded together in the covariance $P_{1,2(C)}$. In contrast, the correlation
190 coefficient $r_{(C)}$ is standardized relative to the scale of each phenotype, providing a more robust
191 quantity for directly predicting and comparing estimates of life history tradeoffs across
192 phenotypes and species. Our model also assumes that phenotypic variances can vary across
193 environmental contexts, but no predictions are made on this variation. Greater plasticity is
194 instead expected in the strength of tradeoff expression caused by fluctuating environmental
195 factors (e.g., environmental harshness, resource availability, local predator density). See Martin
196 (2023) for further details on relaxing these assumptions to model environmental effects on
197 among- and within-individual variances.

198 ***Non-repeated measures***

199 Estimating **Eq 1** with empirical data requires multiple measurements of the same subjects
200 to effectively partition trait correlations due to sources of among- $\mathbf{P}_{(C)}$ and within-individual $\mathbf{\Sigma}_{(C)}$
201 phenotypic variation, relative to a given window of sampling (i.e., a given environmental context
202 C). Repeated individual measurements are often inconsistent or unavailable in a given
203 environmental context (e.g., a single fecundity measurement for individuals in a given year) in
204 long-term field studies, which otherwise provide invaluable datasets for investigating context-
205 specific tradeoffs in the wild. Fortunately, we can still take advantage of long-term environmental
206 variation in such studies to detect variation in tradeoff expression without repeated
207 measurements in a given environmental context. This requires simplifying the CRN model to
208 predict observation-level phenotypic associations across environmental contexts.

$$\begin{aligned} \mathbf{z}_1 &= \mathbf{X}_1 \boldsymbol{\beta}_{\mu 1} + \mathbf{o}_{1(C)} \\ \mathbf{z}_2 &= \mathbf{X}_2 \boldsymbol{\beta}_{\mu 2} + \mathbf{o}_{2(C)} \end{aligned} \quad (2)$$

$$\begin{aligned} [\mathbf{o}_{1(C)}, \mathbf{o}_{2(C)}] &\sim \mathbf{N}(\mathbf{0}, \mathbf{P}_{o(C)}) \\ \mathbf{P}_{o(C)} &= \begin{bmatrix} \sigma_{o_1(C)}^2 & r_{o(C)} \sigma_{o_1(C)} \sigma_{o_2(C)} \\ r_{o(C)} \sigma_{o_2(C)} \sigma_{o_1(C)} & \sigma_{o_2(C)}^2 \end{bmatrix} \\ \operatorname{atanh}(r_{o(C)}) &= \mathbf{X}_3 \boldsymbol{\beta}_r \end{aligned}$$

209

210 Here, the lack of repeated measurements mean that we cannot decompose the variance
 211 between among- and within-individual variation. Therefore, $\mathbf{o}_{1(C)} = \boldsymbol{\alpha}_{1(C)} + \boldsymbol{\varepsilon}_{1(C)}$ and $\mathbf{o}_{2(C)} = \boldsymbol{\alpha}_{2(C)} +$
 212 $\boldsymbol{\varepsilon}_{2(C)}$ are observation-level random effects aggregating variation due to among- and within-
 213 individual differences across measurements, within a given environmental context defined by C
 214 (e.g., a given year, position in space, level of resource abundance). Note that the \mathbf{W} matrix from
 215 **Eq 1** is no longer necessary in **Eq 2** in the absence of repeated measurements. As a consequence,
 216 we expect that the observation-level correlation $r_{o(C)}$ between these random effects to reflect
 217 the combined effect of the among- and within-individual correlations between life history traits,
 218 weighted by the geometric mean of their repeatability R (Dingemanse & Dochtermann, 2013;
 219 Searle, 1961).

$$r_{o(C)} = r_{\alpha(C)} \sqrt{\frac{\sigma_{\alpha 1}^2 \sigma_{\alpha 2}^2}{\sigma_{z 1}^2 \sigma_{z 2}^2}} + r_{\varepsilon(C)} \sqrt{\frac{\sigma_{\varepsilon 1}^2 \sigma_{\varepsilon 2}^2}{\sigma_{z 1}^2 \sigma_{z 2}^2}} = r_{\alpha(C)} \sqrt{R_1 R_2} + r_{\varepsilon(C)} \sqrt{(1 - R_1)(1 - R_2)} \quad (3)$$

220

221 Where phenotypic variances are adjusted for the mean effects of $\mathbf{X}_1 \boldsymbol{\beta}_{\mu 1}$ and $\mathbf{X}_2 \boldsymbol{\beta}_{\mu 2}$. We can see
 222 that inferences about among-individual tradeoffs from the non-repeated measures model (**Eq.**
 223 **2**) will be at greatest risk of bias when $\operatorname{sign}(r_{\alpha}) \neq \operatorname{sign}(r_{\varepsilon})$ and $\sqrt{R_1 R_2} \ll \sqrt{(1 - R_1)(1 - R_2)}$.
 224 Figure 1 shows these general relationships across correlation and repeatability ranges, identifying

225 regions of sign bias. Fortunately, researchers will generally be able to judge their risk of inferential
226 bias based on *a priori* knowledge about the repeatability of life history traits, which tends to be
227 medium to high (Dingemanse et al., 2021). For example, observation-level correlations of
228 behavioral traits will tend to be dominated by within-individual associations (Bell et al., 2009;
229 Cauchoix et al., 2018; Holtmann et al., 2017), while morphological associations will tend to be
230 dominated by among-individual variation (Dingemanse et al., 2021). We reiterate that our
231 models consider measurements of the same individuals observed in different contexts as
232 independent (see supplementary materials Section S1). In addition, our model considers no
233 measurement errors, as we are not able to disentangle it from true within-individual variation
234 using non-repeated measures. Such considerations regarding trait repeatability and
235 measurement error should be explicit when interpreting results without repeated measures.

236 ***Hybrid scenarios***

237 Variation in repeated sampling is also likely to occur across phenotypes due to factors such as
238 difficulty of measurement and the rate of trait expression. While a single measure of age at first
239 reproduction or fecundity in a given environmental context may be available per individual,
240 multiple individual measures may be available for traits such as offspring quality. Such scenarios
241 require a hybrid modeling approach. For example, consider a model with a single predictor for
242 an intergenerational tradeoff between fecundity (e.g., clutch size) and offspring quality, but other
243 traits could equally be studied. The model structure for offspring quality \mathbf{z}_1 (depicted as offspring
244 body mass), a gaussian trait, is given by

$$\mathbf{z}_1 = \mathbf{X}_1\boldsymbol{\beta}_{\mu 1} + \mathbf{W}\boldsymbol{\alpha}_{1(c)} + \boldsymbol{\epsilon}_{1(c)} \quad (4.1)$$

245

246 The linear predictor for \mathbf{z}_1 (mass of an offspring of a given mother) in year C includes a year-
 247 specific mother random effect $\boldsymbol{\alpha}_{1(C)}$ and $\boldsymbol{\varepsilon}_{1(C)}$ being the within-brood/litter variance.

248 The model for fecundity \mathbf{z}_2 follows the same basic structure, with a single fecundity measurement
 249 per female per year. We can use a Poisson distribution where we model the expected rate of
 250 offspring production using a log link function, but other distributions could equally be used.

$$\mathbf{z}_2 = \mathbf{X}_2 \boldsymbol{\beta}_{\mu 2} + \boldsymbol{o}_{2(C)} \quad (4.2)$$

251
 252 Without repeated measures, the random effect $\boldsymbol{o}_{2(C)}$ is specified at the observation-level,
 253 accounting for any overdispersion in the Poisson process across measurements of each female.
 254 The context-dependent tradeoff will be estimated between the among-mother random effect in
 255 offspring quality and the observation-level random effect in fecundity.

$$\begin{aligned} & [\boldsymbol{\alpha}_{1(C)}, \boldsymbol{o}_{2(C)}] \sim \mathbf{N}(\mathbf{0}, \mathbf{P}_{(C)}) \quad (4.3) \\ \mathbf{P}_{(C)} = & \begin{bmatrix} \sigma_{\alpha_{1(C)}}^2 & r_{(C)} \sigma_{\alpha_{1(C)}} \sigma_{o_{2(C)}} \\ r_{(C)} \sigma_{\alpha_{1(C)}} \sigma_{o_{2(C)}} & \sigma_{o_{2(C)}}^2 \end{bmatrix} \\ & \operatorname{atanh}(r_{(C)}) = \mathbf{X}_3 \boldsymbol{\beta}_r \end{aligned}$$

256
 257 Reducing **Eq. 3**, the correlation r_C between the individual- $\boldsymbol{\alpha}_{1(C)}$ and observation-level $\boldsymbol{o}_{2(C)}$ effects
 258 will necessarily be proportional to the among-individual correlation across life history traits.

$$r_{o(C)} = r_{\alpha(C)} \sqrt{\frac{\sigma_{\alpha 2}^2}{\sigma_{z 2}^2}} = r_{\alpha(C)} \sqrt{R_2} \quad (5)$$

259
 260 Note that this method does not allow the inclusion of non-continuous traits (e.g., Bernoulli traits)
 261 in the absence of repeated measurements within a given environmental context C (e.g., a given
 262 year).

263

264 Validation on simulated datasets

265 We validated the CRN model on two different types of tradeoffs. First, we used the hybrid CRN
266 model to study an intergenerational tradeoff between fecundity and quality. The hybrid model
267 is well suited because fecundity (i.e., clutch/litter size) has a single measurement per mother per
268 year, while offspring quality (i.e., offspring mass) has repeated measurements per mother per
269 year (one measurement for each offspring produced). Second, we used the non-repeated
270 measures CRN model to study an intraindividual tradeoff between fecundity (clutch/litter size)
271 and parental growth (the change of mass from a year to the next). The non-repeated measures
272 CRN model is well suited as both traits are expressed only a single time per year (one fecundity
273 and one parental growth measure per individual per year). Note that tradeoffs are described as
274 intergenerational or intraindividual depending on which traits are studied (as explained in
275 Stearns, 1989), and both type of tradeoff can be decomposed into among- and within-individual
276 covariation. We simulate data for these two tradeoffs using the individual-based simulation
277 described in Bliard et al. (2024), whereby the among-individual correlation between life history
278 traits can be made dependent on the environmental context. The code to generate data from
279 the individual-based simulation can be found on github
280 (https://github.com/lbiard/detecting_tradeoffs_crn_models). This model validation is only
281 intended to show that context-dependent among-individual correlations (i.e., context dependent
282 tradeoffs) can be successfully recovered. For a more extensive simulation-based calibration of
283 CRN models over a broad range of parameter values, see Martin (2023).

284 ***Intergenerational tradeoff (offspring quantity-quality)***

285 We first focused on an intergenerational tradeoff between offspring quantity and quality (hybrid
286 CRN model). This quantity-quality tradeoff has been the focus of numerous studies since Lack's
287 pioneering work on bird clutch sizes (Einum & Fleming, 2000; Fischer et al., 2011; Gillespie et al.,
288 2008; Lack, 1947; Williams, 1966). We simulate 30 years of individual-based data in which 25 new
289 individuals enter the population each year, reproduce with an average clutch/litter size of 2.5,
290 and then have a probability to survive to next year of 0.6. This yielded a final simulated dataset
291 of 750 individuals, totaling 1578 reproductive events and 4783 offspring. An observation-level
292 correlation was included between offspring mass and clutch size, and this correlation was made
293 dependent on a single climatic predictor. The same climatic predictor was also included to
294 influence both clutch size and offspring mass.

295 ***Intraindividual tradeoff (fecundity-growth)***

296 We then simulated data for an intraindividual tradeoff between fecundity and growth (non-
297 repeated measures CRN model). This simulated dataset is also made of 30 years and 750
298 individuals, for a total of 1974 reproductive events, with a variable observation-level correlation
299 between individual growth and fecundity, which is itself dependent on a single climatic predictor.

300

301 Study systems and application on empirical datasets

302 ***Marmots***

303 We applied the hybrid CRN model (one trait with repeated individual measurements within a
304 year and one trait without) on data from a yellow-bellied marmot population monitored at the
305 Rocky Mountain Biological Laboratory in Gothic, Colorado (38°57'N, 106°59'W) during the
306 summer season each year, whereby extensive individual-based data is collected (Armitage, 2014;

307 Blumstein, 2013). In Alpine marmots *Marmota marmota*, an offspring quality-quantity tradeoff
308 has been found (Berger et al., 2015), while it remained mostly elusive in yellow-bellied marmots,
309 being only found for older mothers (Kroeger et al., 2020), whereby within-cohort selection has
310 likely reduced the amount of among-individual variance in resource acquisition, thus making the
311 tradeoff visible (Kendall et al., 2011; van Noordwijk & de Jong, 1986). Therefore, we searched for
312 an intergenerational tradeoff between mothers' fecundity and offspring estimated mass
313 (offspring quality-quantity tradeoff). We used repeated measurements of offspring mass for each
314 mother (one mass estimate for each offspring in a given litter). The offspring weaning mass was
315 imputed based on the date of emergence for each litter and mass measurements from captures
316 later in the season, following the method of Ozgul et al. (2010). We considered two measures
317 quantifying environmental conditions for a given year. First, the total amount of snow during the
318 preceding winter, with years of little overwinter snow considered harsher for marmots as it offers
319 limited thermal insulation during the hibernation (Barash, 1973; Cordes et al., 2020; Wells et al.,
320 2022). Second, the average daily maximum temperature during the month of June, with warmer
321 summer temperatures considered unfavorable conditions for marmots as they are prone to
322 overheating, hence limiting the time that can be allocated to foraging (Cordes et al., 2020; Krajick,
323 2004; Melcher et al., 1990). Note that we used temperature in June and not July as commonly
324 used in this system (Cordes et al., 2020), because this is more likely to represent the conditions
325 experienced for most offspring before emergence and weaning, since most offspring emerge in
326 July. We expected tradeoffs to be more strongly expressed among individuals in years with little
327 overwinter snow or high summer temperature. In total, we used 2540 offspring mass from 597
328 reproductive events, from 279 females across 42 years.

329 We modeled offspring mass using a normal distribution (**Eq. 6.1**), and we included as
 330 covariates (i.e., in \mathbf{X}_1) the total amount of snow during the winter, June average maximum
 331 temperature, age of the mother and its quadratic effect, and mother's estimated mass in early
 332 June as a proxy of mother's quality. A year random effect δ_1 was also included.

$$\text{offspring mass} = \mathbf{X}_1\boldsymbol{\beta}_1 + \delta_1 + \mathbf{W}\boldsymbol{\alpha}_{1(Y)} + \boldsymbol{\epsilon}_{1(Y)} \quad (6.1)$$

333 With $\boldsymbol{\alpha}_{1(Y)}$ being a year-specific mother random effect and $\boldsymbol{\epsilon}_{1(Y)}$ the within-litter variance.
 334 We modeled the second trait, fecundity (i.e., litter size), using a Poisson distribution (**Eq. 6.2**), as
 335 a function of the same covariates (\mathbf{X}_2), except June average maximum temperature, since it
 336 cannot affect fecundity as pregnancies mostly occur before this period. A year random effect δ_2
 337 was also included.
 338

$$\log(\text{litter size}) = \mathbf{X}_2\boldsymbol{\beta}_2 + \delta_2 + \boldsymbol{o}_{2(Y)} \quad (6.2)$$

339 For the observation-level correlation (**Eq. 6.3**), the two environmental variables (winter snow and
 340 June temperature) were added as covariates (\mathbf{X}_3).
 341

$$\begin{aligned} & [\boldsymbol{\alpha}_{1(Y)}, \boldsymbol{o}_{2(Y)}] \sim \mathbf{N}(\mathbf{0}, \mathbf{P}^{(Y)}) \quad (6.3) \\ & \mathbf{P}^{(Y)} = \begin{bmatrix} \sigma_{\alpha_1(Y)}^2 & r^{(X)} \sigma_{\alpha_1(Y)} \sigma_{o_2(Y)} \\ r^{(Y)} \sigma_{\alpha_1(Y)} \sigma_{o_2(Y)} & \sigma_{o_2(Y)}^2 \end{bmatrix} \\ & \text{atanh}(r^{(Y)}) = \mathbf{X}_3\boldsymbol{\beta}_3 \end{aligned}$$

342 We performed posterior predictive checks, showing a good concordance between the litter size
 343 data, and data generated under the model (see Figure S3). However, the model slightly
 344 underestimates the variance in offspring mass. Overall, posterior predictive checks highlight that
 345

346 the use of a Normal distribution to model offspring mass, and a Poisson distribution with an
347 observation random effect to model litter size, were appropriate in this system.

348

349 ***Soay sheep***

350 We applied the non-repeated measures CRN model on Soay sheep data, as we have no repeated
351 individual measurement within a given year available for neither of the traits studied. We used
352 data from an unmanaged population of feral sheep in the Village Bay area of the island of Hirta
353 (57°48'N, 8°37'W), which has been monitored since 1985 (Clutton-Brock & Pemberton, 2004). In
354 Soay sheep, survival costs of reproduction were found for breeding ewes, particularly in
355 populations at high densities or following stormy winters (Tavecchia et al., 2005). Therefore, we
356 searched for an intraindividual tradeoff between ewes' fecundity defined as the number of lambs
357 born in Spring (ranging from 0 to 2) and their log mass in the following summer, with both traits
358 conditional on ewes surviving the winter. We considered two environmental variables to
359 characterize the ecological harshness faced by the sheep in a given year: population density and
360 NAO (North Atlantic Oscillation) in the winter preceding parturition, with high NAO values
361 corresponding to wet and stormy winters (Coulson et al., 2001; Regan et al., 2022). In total, we
362 used data from 2497 reproductive events across 37 years, for 861 ewes with known mass in the
363 summer preceding the reproductive event, as well as known mass in the following summer. We
364 expected tradeoffs to be more strongly expressed in years of high population density or high
365 NAO.

366 As ewes' fecundity in a given year is restricted to [0,2], we could not use a Poisson
367 regression. This is due to the count data being underdispersed relative to a Poisson distribution.

368 We therefore modeled the ewe's fecundity using an ordinal regression (also called cumulative
 369 logistic regression; **Eq. 7.1**), and we included as covariates (\mathbf{X}_1) the individual's log mass preceding
 370 the reproductive event as a proxy of quality, age and its quadratic effect, and population density.

$$\text{logit}(\Pr(\mathbf{N}_{\text{offspring}} \leq i)) = \theta_i - (\mathbf{X}_1\boldsymbol{\beta}_1 + \boldsymbol{\delta}_1 + \boldsymbol{o}_{1(Y)}) \quad (7.1)$$

371
 372 Where the cumulative probability of having at most i offspring is given as a function of the
 373 threshold θ_i and the matrix of covariates \mathbf{X}_1 , as well as a year random effect $\boldsymbol{\delta}_1$ and a year specific
 374 observation random effect $\boldsymbol{o}_{1(Y)}$.

375 We modeled the ewe's log mass in the following summer using a normal distribution (**Eq. 7.2**),
 376 and included in \mathbf{X}_2 the same covariates as in \mathbf{X}_1 , as well as NAO in the winter preceding parturition.
 377 A year random effect $\boldsymbol{\delta}_2$ was also included.

$$\mathbf{mass} = \mathbf{X}_2\boldsymbol{\beta}_2 + \boldsymbol{\delta}_2 + \boldsymbol{o}_{2(Y)} \quad (7.2)$$

378
 379 For the observation-level correlation (**Eq. 7.3**), the two ecological variables (winter NAO and
 380 density) were added as covariates (\mathbf{X}_3).

$$\begin{aligned} & [\boldsymbol{\alpha}_{1(Y)}, \boldsymbol{o}_{2(Y)}] \sim N(\mathbf{0}, \mathbf{P}^{(Y)}) \quad (7.3) \\ & \mathbf{P}^{(Y)} = \begin{bmatrix} \sigma_{\alpha_1(Y)}^2 & r^{(Y)} \sigma_{\alpha_1(Y)} \sigma_{o_2(Y)} \\ r^{(Y)} \sigma_{\alpha_1(Y)} \sigma_{o_2(Y)} & \sigma_{o_2(Y)}^2 \end{bmatrix} \\ & \text{atanh}(r^{(Y)}) = \mathbf{X}_3\boldsymbol{\beta}_3 \end{aligned}$$

381
 382 The posterior predictive checks we performed highlighted a good fit between the data and data
 383 generated under the model. This confirms that using a normal distribution to model ewe's mass,
 384 and using a cumulative logistic regression to model ewe's number of offspring, were appropriate
 385 (see Figure S4).

386

387 Model implementation

388 We implemented all multivariate models described above in a Bayesian framework using the Stan
389 statistical language (Carpenter et al., 2017), through the software R (R Core Team, 2021) using
390 the R package *CmdStanR* (Gabry & Češnovar, 2020). Stan was preferred for model
391 implementation because of its flexibility. Common regularizing priors were used for all model
392 parameters: normal distributions of mean 0 and standard deviation of 1 for intercepts and slopes
393 coefficients, and exponential distributions of rate 2 for variance parameters. Each model ran on
394 3 chains, with a burn-in period of 1000 iterations, sampling for 3000 iterations, keeping all the
395 sampled iterations (Link & Eaton, 2012). Convergence of parameter estimates was assessed
396 visually and using the Gelman-Rubin diagnostic (Gelman & Rubin, 1992). We report the full
397 posterior distributions, alongside their mean, 50%, and 89% credible intervals (McElreath, 2020).
398 The Stan code to implement all the CRN models presented in this study is archived on GitHub
399 (https://github.com/lbiard/detecting_tradeoffs_crn_models) and Zenodo
400 (<https://doi.org/10.5281/zenodo.12800618>).

401

402 **Results**

403 The model validation performed on simulated datasets showed that parameters were correctly
404 recovered for both intergenerational tradeoffs (Figure 2) and intraindividual tradeoffs (Figure 3).
405 While these simulation examples do not quantify bias of estimations (more details from a
406 simulation-based calibration of CRN models are available in Martin (2023)), they still confirm that

407 the model presented in the methods is able to detect context-dependence in the expression of
408 tradeoffs.

409 The model applied to yellow-bellied marmot data shows trends towards tradeoffs being
410 more strongly expressed in years with harsh environmental conditions, albeit with high
411 uncertainty in the estimates (Figure 4). We found a positive mean effect of the amount of
412 overwinter snow on the correlation (Figure 4), meaning that the tradeoff between fecundity and
413 offspring quality was more strongly expressed after winters with little snow. We also found a
414 negative mean effect of the average maximum June temperature on the correlation (Figure 4),
415 where females with more offspring were more likely to have lighter offspring during warmer
416 summers. Estimated effects of covariates on either fecundity or offspring mass can be found in
417 Figure 4, as well as in Figure S5.

418 Estimated effects of covariates on the correlation also had high uncertainty in the Soay
419 sheep dataset (Figure 5). Overall, we found that the correlation tended to be negative across
420 most environments, which means that ewe's growth was lower for the ones that weaned
421 offspring (Figure 5). Contrary to our expectations, while we hypothesized that the tradeoffs
422 should be more strongly expressed in wet and stormy winters (high NAO index), we found a
423 positive effect of winter NAO on the correlation between fecundity and growth (Figure 5). We
424 also found a positive effect of population density on the expression of the tradeoff (Figure 5).
425 Estimated effects of covariates on either fecundity or ewe's mass can be found in Figure 5, as
426 well as in Figure S6.

427

428

Discussion

429 Our proof-of-concept study demonstrates that hierarchical multivariate CRN models (Martin,
430 2023) can be used successfully to detect and estimate context-dependent changes in tradeoff
431 expression, though estimation uncertainty can be large. In agreement with theoretical
432 predictions and despite large uncertainty, we found that reproductive tradeoffs in yellow-bellied
433 marmots tend to be more strongly expressed under unfavorable climatic conditions. In Soay
434 sheep, we found some context-dependence in the expression of the tradeoff, but effect
435 directions were opposite to our initial prediction. This hierarchical model has the potential to be
436 used on many long-term individual-based datasets and could help improve our understanding of
437 tradeoff expression and life history theory.

438 Although the initial motivation to use this method partly rested on the observed difficulty
439 of finding tradeoffs in empirical datasets, we found that in both sheep and marmots, the
440 tradeoffs tend to be expressed across most environments, with mean phenotypic correlations
441 being negative overall. Thus, ironically, in these two empirical datasets, tradeoffs might have
442 been detected using simpler multivariate methods without the need for context dependence.
443 However, this should not come as a surprise for Soay sheep, as this negative correlation between
444 growth and fecundity was already found on a smaller dataset (Fung et al., 2022). Nonetheless,
445 the results still highlight that context-dependence has the potential to hinder our ability to detect
446 tradeoffs in some cases. For instance, when marmots experience favorable environmental
447 conditions, the average correlation is closer to null with credibility intervals nearing or
448 overlapping zero (Figure 4), while this intergenerational tradeoff is found to be more strongly
449 expressed during harsh years. In Soay sheep, context dependence appears to be marked for the
450 expression of the tradeoff, but opposite to our predictions. Indeed, we found a positive

451 correlation between growth and fecundity only under the harshest environmental conditions
452 (high population density and high winter NAO, Figure 5). Since ewes' mass is measured in the
453 following summer and not directly after parturition, harsh winter conditions are expected to
454 increase overwinter mortality (Milner et al., 1999), lowering spring population density and
455 reducing competition. This could potentially help surviving ewes to recover their body condition
456 between spring and summer, which is the period of greatest grass growth, hence potentially
457 explaining our counter-intuitive results. We can also speculate that the result could have arisen
458 from two potential pitfalls due to idiosyncrasies of the Soay sheep data. First, among-individual
459 variation in fecundity is limited in sheep, ranging from no offspring to twins, potentially making
460 it more complicated for the model to estimate variances accurately (Fay, Authier, et al., 2022;
461 Kain et al., 2015). Second, both ewes' growth and fecundity are conditional on survival in the
462 data, hence individuals who suffered most from the cost of reproduction and did not survive are
463 not present in the analysis, potentially biasing the results (Hadfield, 2008). Finally, while we
464 expected more negative phenotypic correlations under harsh conditions, where among-
465 individual variance in resource allocation is greater than among-individual variance in acquisition,
466 it is theoretically possible that in population facing adverse conditions, a few robust individuals
467 monopolize most resources, thus increasing the among-individual variance in resource
468 acquisition (Chambert et al., 2013), hence leading to positive estimates of phenotypic
469 correlations.

470 Despite the potential of this modeling approach to study context-dependent tradeoffs, a
471 few methodological limitations are to be considered. A recent study conducted by Fay et al.
472 (2022) highlighted that multivariate models with correlated random effects for Bernoulli traits

473 performed rather poorly, resulting in a potentially large bias and imprecise estimates of variances
474 and covariances. This is in part because Bernoulli traits contain less information than continuous
475 variables, making estimations of variances complicated (Fay, Authier, et al., 2022), but also
476 because the data available to estimate individual heterogeneity is usually scarce (Browne et al.,
477 2007). The model we present suffers from this limitation, and even more so when there is only a
478 single individual observation per individual per sampling occasion (e.g., parental survival), and
479 when the trait is not repeatable (death can only occur once). This issue renders the model, as
480 well as any other multilevel model, unable to meaningfully estimate distinct mean and variance
481 parameters for Bernoulli traits, due to the fact that the mean p of a Bernoulli variable determines
482 its variability $p(1-p)$ without scope for overdispersion. Therefore, environmental effects on the
483 mean of Bernoulli measures will necessarily change their variances (Skrondal & Rabe-Hesketh,
484 2007). However, when repeated Bernoulli observations or a binomial measure are available
485 within each sampling occasion (e.g., survival of each offspring within a litter), the CRN model can
486 then be used to partition distinct environmental effects on trait means and (co)variances. As we
487 have shown in the present study, despite this limitation, the CRN remains applicable to single
488 measures of continuous traits and count measures (e.g., growth, fecundity, phenology,
489 behavioral traits), as well as proportions and various other kinds of non-Gaussian measures.
490 Another limitation of the proposed method is that sample sizes needed are likely to be large,
491 with enough individuals in each environmental context, and importantly enough sampling
492 occasions across which to estimate the context dependence of tradeoff expression. Nonetheless,
493 many long-term individual-based studies should have enough data to fulfill these requirements
494 (de Villemereuil et al., 2020).

495 Despite the abovementioned caveats and limitations of the methodology in the absence
496 of repeated measurements, this new model is a development that could be useful for many
497 datasets. Thanks to its implementation in a Bayesian framework using Stan (Carpenter et al.,
498 2017), it offers great flexibility and can be easily repurposed and modified to fit the idiosyncrasies
499 of a given dataset or species life history. It is also straightforward to extend the model by adding
500 a pedigree for quantitative genetic analysis (see Martin, 2023), even though phenotypic
501 correlations should be good approximations of genetic correlations in most cases (Cheverud,
502 1988; Dochtermann, 2011; Roff, 1995). While we presented a bivariate model, this model is not
503 necessarily limited to two traits, and more continuous traits and their covariances could also be
504 analyzed simultaneously. We also restricted our proof-of-concept study to the reaction norm of
505 the correlation between traits, but researchers interested in the canalization of traits variances
506 as a response to the environmental context could also benefit from this modeling approach
507 (Péron et al., 2016).

508 Life history tradeoffs have long been sought after, but difficult to detect in observational
509 data due to individual heterogeneity (Metcalf, 2016; Reznick et al., 2000; van Noordwijk & de
510 Jong, 1986). Previous studies have also highlighted that life history tradeoffs could be expressed
511 only under unfavorable ecological conditions (Cohen et al., 2020; Stearns, 1989). Yet, despite our
512 knowledge of the issues hindering tradeoff detection, we still lacked a statistical framework that
513 permits the detection of context-dependence in tradeoff expression. Our proof-of-concept study
514 shows that this context dependence can be detected. This method has the potential to be applied
515 by demographers and evolutionary ecologists having long-term individual-based datasets at
516 hands, with many study systems having the required data (Culina et al., 2021; de Villemereuil et

517 al., 2020). Altogether, this method has the potential to help us improve our understanding of life
518 history theory, and in part resolve van Noordwijk and de Jong's (1986) conundrum of tradeoff
519 detection, by accounting for the context-dependence of their expression.

520

521 **Acknowledgements**

522 This work was supported by a Swiss National Science Foundation Grant (31003A_182286 to A.O).

523 We thank Billy Barr for the long-term collection of snow data at RMBL, and all the people who

524 helped collect data on marmots and sheep over the years. Most recently, marmots were studied

525 with support from the US National Science Foundation (D.E.B.-1119660 and 1557130 to D.T.B.).

526 The St Kilda Soay sheep project has been largely funded by the UK's Natural Environment

527 Research Council (NERC), and is indebted to many project members and volunteers; the National

528 Trust for Scotland for permission to work on St Kilda and QinetiQ and Kilda Cruises for logistical

529 support in the field. We thank the editor, an anonymous reviewer, and Remi Fay for useful

530 comments and suggestions.

531 **Authors contributions**

532 LB, JSM, AO, MP, DZC conceived the study. JSM designed the initial modeling framework and LB

533 analyzed the data. DTB, JGAM, JMP, DHN collected and curated the data. LB and JSM wrote the

534 first draft with input from AO, MP, DZC. All authors contributed to the editing of the manuscript.

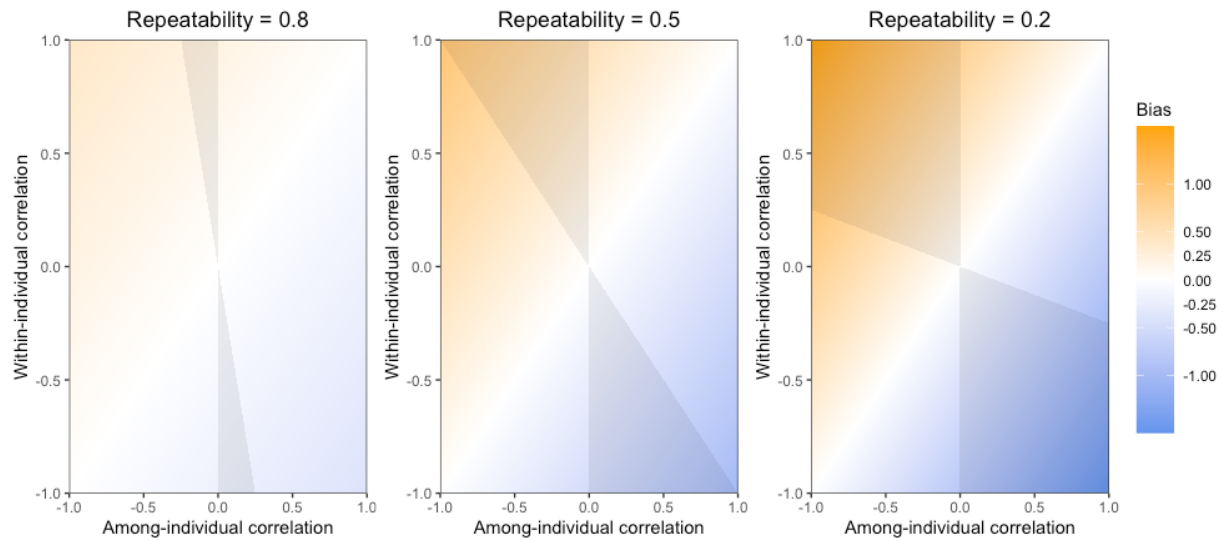
535 **Data and code availability**

536 The data, as well as the R and Stan code necessary to reproduce the results are available on

537 GitHub https://github.com/lbiard/detecting_tradeoffs_crn_models and are archived on Zenodo

538 <https://doi.org/10.5281/zenodo.12800618>.

539 **Figures**



540

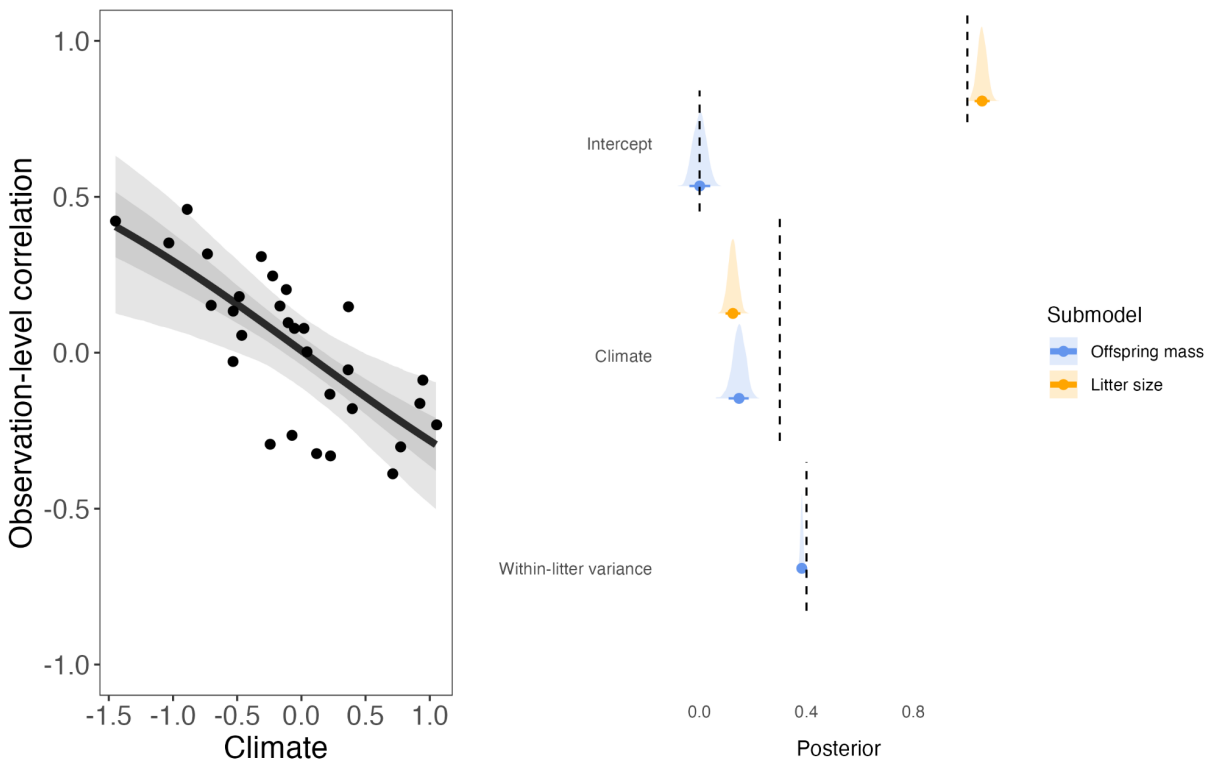
541 Figure 1: General relationships across correlations and repeatability ranges based on **Eq 3** for a
542 non-repeated measures CRN (model of **Eq 2**), identifying the magnitude of correlation bias and
543 the regions of sign bias. The bias is here defined as the difference between the observation-level
544 correlation and the among-individual correlation, using the latter as a reference. Parameter
545 spaces in gray represent the regions of sign bias, where the observation-level correlation has a
546 sign opposite to the among-individual correlation. This highlights that the observation-level
547 correlation is mostly influenced by the among-individual correlation for traits with high
548 repeatability, while it is mostly influenced by the within-individual correlation for traits with low
549 repeatability.

550

551

552

553



554

555 Figure 2: Left panel: estimated vs. simulated observation-level correlation between litter size and
 556 offspring mass as a function of climate, after accounting for the effect of climate on both traits.

557 The regression line indicates the mean effect of climate on the correlation, while the shaded
 558 areas depict the 50% and 89% credible intervals predicted by the model. Each black dot

559 represents the simulated observation-level correlation between both traits in a given year

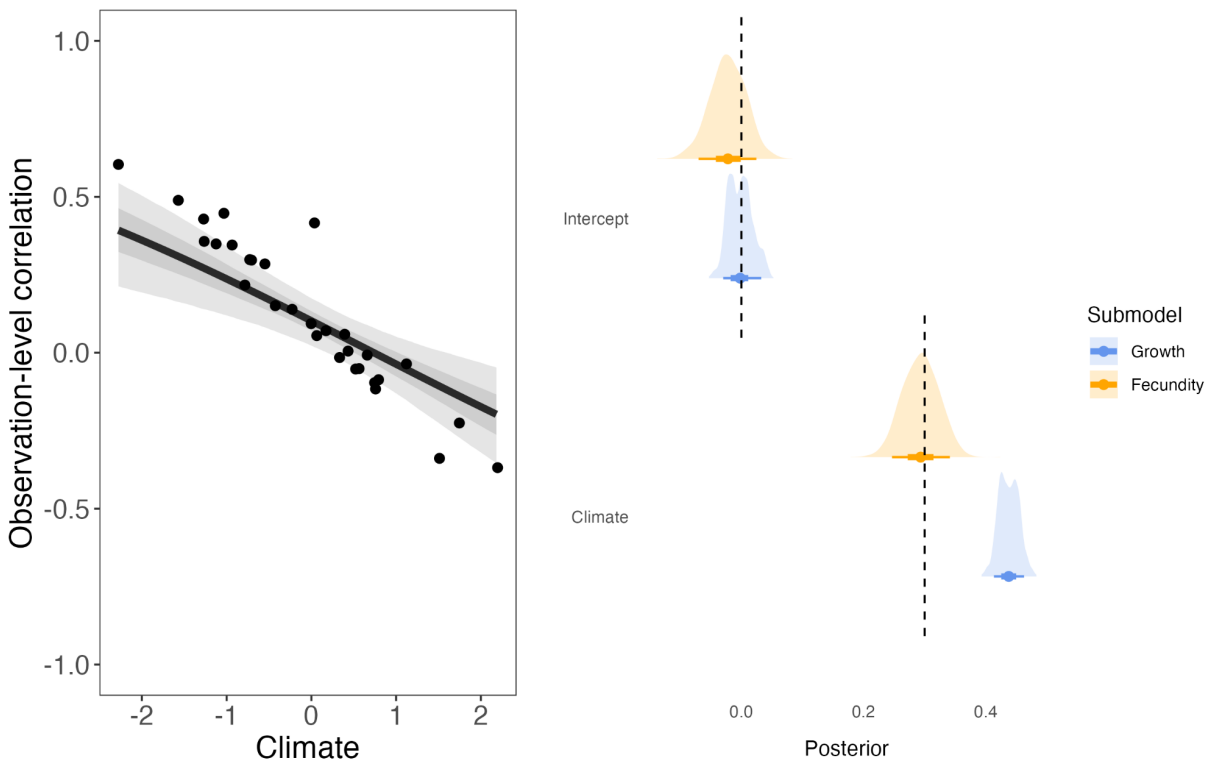
560 depending on climate. Right panel: estimated vs. simulated intercepts and slopes for the

561 offspring mass and litter size sub-models. Dashed lines represent the value used to simulate the
 562 data, while the distributions and intervals represent the posterior distributions estimated by the

563 model, alongside the median, 50%, 89% credible intervals. Litter size estimates are presented on

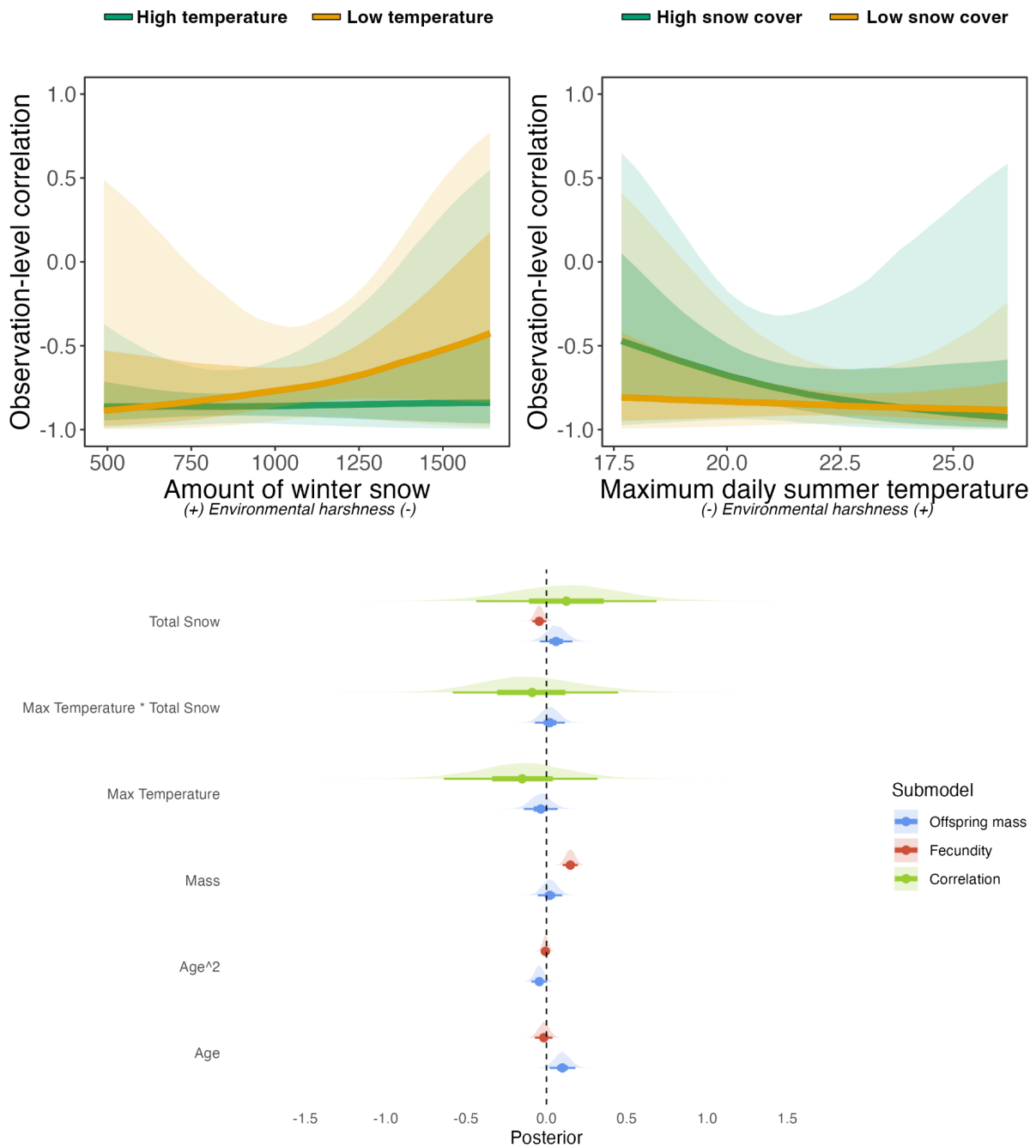
564 the log scale.

565



566

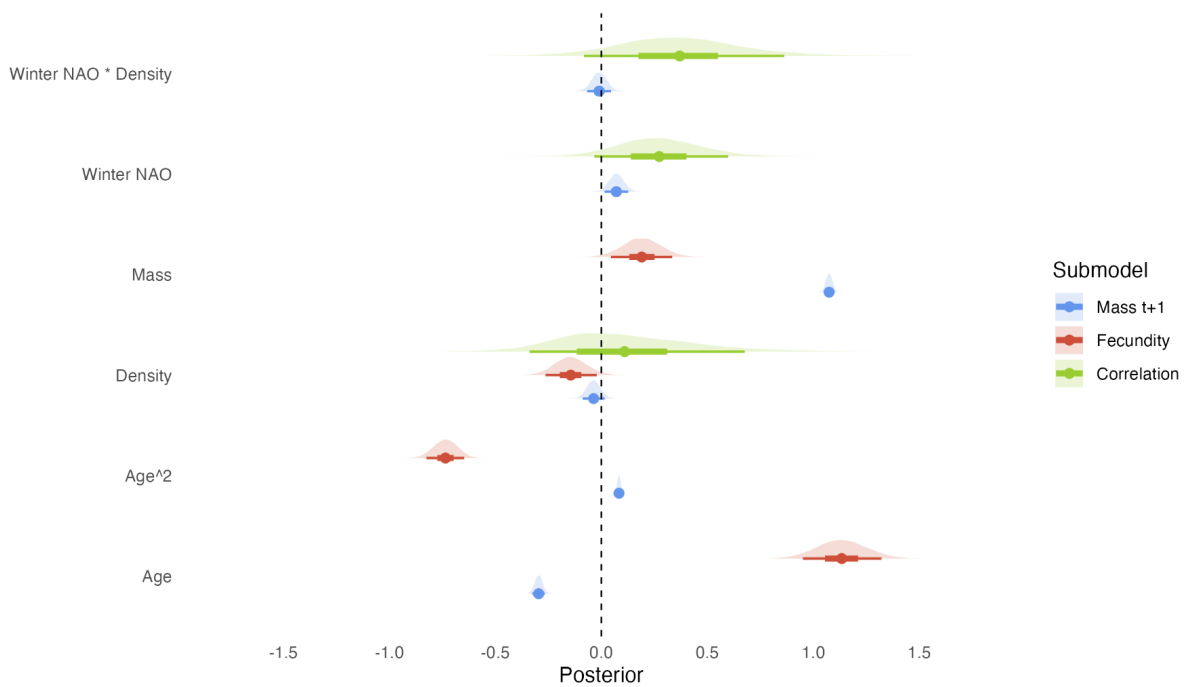
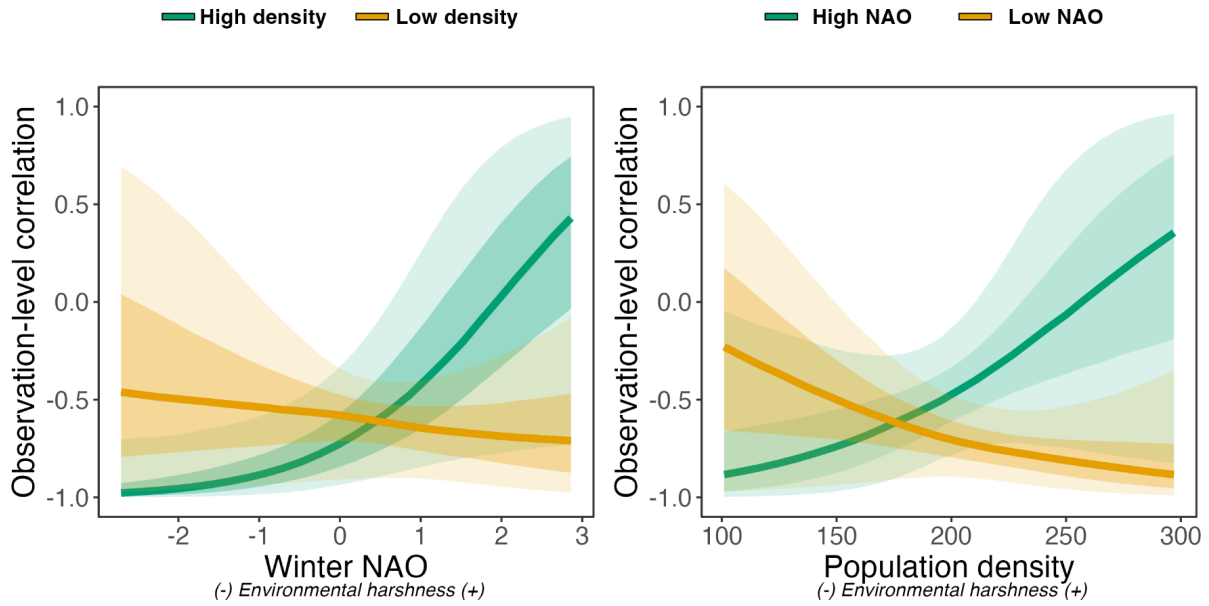
567 Figure 3: Left panel: estimated vs. simulated observation-level correlation between fecundity and
 568 growth as a function of climate, after accounting for the effect of climate on both traits. The
 569 regression line indicates the mean effect of climate on the correlation, while the shaded areas
 570 depict the 50% and 89% credible intervals predicted by the model. Each black dot represents the
 571 simulated observation-level correlation between both traits in a given year depending on climate.
 572 Right panel: estimated vs. simulated intercepts and slopes for the growth and fecundity sub-
 573 models. Dashed lines represent the value used to simulate the data, while the distributions and
 574 intervals represent the posterior distributions estimated by the model, alongside the median,
 575 50%, 89% credible intervals. Fecundity estimates are presented on the log scale.



576

577 Figure 4: Observation-level correlation between litter size and offspring mass in marmots as a
 578 function of the total amount of snow in the preceding winter at high and low temperature (top
 579 left panel) and the maximum daily June temperature of the year at high and low snow cover (top
 580 right panel). Estimated effects of standardized predictors (bottom panel) on offspring mass,

581 fecundity, and the observation-level correlation between both traits in marmots. The regression
 582 line indicates the median estimated effect, while the shaded areas depict the 50% and 89%
 583 credible intervals predicted by the model.



585 Figure 5: Observation-level correlation between fecundity and mothers' mass in the following
586 year in Soay sheep as a function of the winter NAO at high and low density (top left panel), and
587 as a function of the population density at high and low winter NAO values (top right panel).
588 Estimated effects (bottom panel) of standardized predictors on mother's mass in the following
589 year, fecundity, and the observation-level correlation between both traits in Soay sheep. The
590 figure displays the posterior distributions estimated by the model, alongside the median, 50%,
591 and 89% credible intervals.

592

593

594

595

596

597

598

599

600

601

602

603

604

605

606

607 **References**

- 608 Agrawal, A. A. (2020). A scale-dependent framework for trade-offs, syndromes, and
609 specialization in organismal biology. *Ecology*, *101*(2), e02924.
610 <https://doi.org/10.1002/ecy.2924>
- 611 Armitage, K. B. (2014). *Marmot Biology: Sociality, Individual Fitness, and Population Dynamics*.
612 Cambridge University Press. <https://doi.org/10.1017/CBO9781107284272>
- 613 Barash, D. P. (1973). The Social Biology of the Olympic Marmot. *Animal Behaviour Monographs*,
614 *6*, 171–245. [https://doi.org/10.1016/0003-3472\(73\)90002-X](https://doi.org/10.1016/0003-3472(73)90002-X)
- 615 Bell, A. M., Hankison, S. J., & Laskowski, K. L. (2009). The repeatability of behaviour: A meta-
616 analysis. *Animal Behaviour*, *77*(4), 771–783.
617 <https://doi.org/10.1016/j.anbehav.2008.12.022>
- 618 Berger, V., Lemaître, J.-F., Gaillard, J.-M., & Cohas, A. (2015). How do animals optimize the size-
619 number trade-off when aging? Insights from reproductive senescence patterns in
620 marmots. *Ecology*, *96*(1), 46–53. <https://doi.org/10.1890/14-0774.1>
- 621 Bielby, J., Mace, G. M., Bininda-Emonds, O. R. P., Cardillo, M., Gittleman, J. L., Jones, K. E.,
622 Orme, C. D. L., & Purvis, A. (2007). The Fast-Slow Continuum in Mammalian Life History:
623 An Empirical Reevaluation. *The American Naturalist*, *169*(6), 748–757.
624 <https://doi.org/10.1086/516847>
- 625 Bliard, L., Paniw, M., Childs, D. Z., & Ozgul, A. (2024). Population dynamic consequences of
626 context-dependent tradeoffs across life histories. *The American Naturalist*, *203*(6), 681–
627 694. <https://doi.org/10.1086/730111>
- 628 Blumstein, D. T. (2013). Yellow-bellied marmots: Insights from an emergent view of sociality.

629 *Philosophical Transactions of the Royal Society B: Biological Sciences*, 368(1618),
630 20120349. <https://doi.org/10.1098/rstb.2012.0349>

631 Browne, W. J., McCleery, R. H., Sheldon, B. C., & Pettifor, R. A. (2007). Using cross-classified
632 multivariate mixed response models with application to life history traits in great tits
633 (Parus major). *Statistical Modelling*, 7(3), 217–238.
634 <https://doi.org/10.1177/1471082X0700700301>

635 Cam, E., Link, W. A., Cooch, E. G., Monnat, J., & Danchin, E. (2002). Individual Covariation in
636 Life-History Traits: Seeing the Trees Despite the Forest. *The American Naturalist*, 159(1),
637 96–105. <https://doi.org/10.1086/324126>

638 Carpenter, B., Gelman, A., Hoffman, M. D., Lee, D., Goodrich, B., Betancourt, M., Brubaker, M.,
639 Guo, J., Li, P., & Riddell, A. (2017). Stan: A Probabilistic Programming Language. *Journal*
640 *of Statistical Software*, 76, 1–32. <https://doi.org/10.18637/jss.v076.i01>

641 Cauchoix, M., Chow, P. K. Y., van Horik, J. O., Atance, C. M., Barbeau, E. J., Barragan-Jason, G.,
642 Bize, P., Boussard, A., Buechel, S. D., Cabirol, A., Cauchard, L., Claidière, N., Dalesman, S.,
643 Devaud, J. M., Didic, M., Doligez, B., Fagot, J., Fichtel, C., Henke-von der Malsburg, J., ...
644 Morand-Ferron, J. (2018). The repeatability of cognitive performance: A meta-analysis.
645 *Philosophical Transactions of the Royal Society B: Biological Sciences*, 373(1756),
646 20170281. <https://doi.org/10.1098/rstb.2017.0281>

647 Chambert, T., Rotella, J. J., Higgs, M. D., & Garrott, R. A. (2013). Individual heterogeneity in
648 reproductive rates and cost of reproduction in a long-lived vertebrate. *Ecology and*
649 *Evolution*, 3(7), 2047–2060. <https://doi.org/10.1002/ece3.615>

650 Chang, C., Moiron, M., Sánchez-Tójar, A., Niemelä, P. T., & Laskowski, K. L. (2023). What is the

651 meta-analytic evidence for life-history trade-offs at the genetic level? *Ecology Letters*,
652 ele.14354. <https://doi.org/10.1111/ele.14354>

653 Cheverud, J. M. (1988). A Comparison of Genetic and Phenotypic Correlations. *Evolution*, 42(5),
654 958–968. <https://doi.org/10.1111/j.1558-5646.1988.tb02514.x>

655 Clutton-Brock, T. H., & Pemberton, J. M. (2004). *Soay Sheep Dynamics and Selection in an Island*
656 *Population*. Cambridge University Press.

657 Cohen, A. A., Coste, C. F. D., Li, X.-Y., Bourg, S., & Pavard, S. (2020). Are trade-offs really the key
658 drivers of ageing and life span? *Functional Ecology*, 34(1), 153–166.
659 <https://doi.org/10.1111/1365-2435.13444>

660 Compagnoni, A., Bibian, A. J., Ochocki, B. M., Rogers, H. S., Schultz, E. L., Sneek, M. E., Elderd, B.
661 D., Iler, A. M., Inouye, D. W., Jacquemyn, H., & Miller, T. E. X. (2016). The effect of
662 demographic correlations on the stochastic population dynamics of perennial plants.
663 *Ecological Monographs*, 86(4), 480–494. <https://doi.org/10.1002/ecm.1228>

664 Cordes, L. S., Blumstein, D. T., Armitage, K. B., CaraDonna, P. J., Childs, D. Z., Gerber, B. D.,
665 Martin, J. G. A., Oli, M. K., & Ozgul, A. (2020). Contrasting effects of climate change on
666 seasonal survival of a hibernating mammal. *Proceedings of the National Academy of*
667 *Sciences*, 117(30), 18119–18126. <https://doi.org/10.1073/pnas.1918584117>

668 Coulson, T., Catchpole, E. A., Albon, S. D., Morgan, B. J. T., Pemberton, J. M., Clutton-Brock, T.
669 H., Crawley, M. J., & Grenfell, B. T. (2001). Age, Sex, Density, Winter Weather, and
670 Population Crashes in Soay Sheep. *Science*, 292(5521), 1528–1531.
671 <https://doi.org/10.1126/science.292.5521.1528>

672 Cressler, C. E., Bengtson, S., & Nelson, W. A. (2017). Unexpected Nongenetic Individual

673 Heterogeneity and Trait Covariance in *Daphnia* and Its Consequences for Ecological and
674 Evolutionary Dynamics. *The American Naturalist*, 190(1), E13–E27.
675 <https://doi.org/10.1086/691779>

676 Culina, A., Adriaensen, F., Bailey, L. D., Burgess, M. D., Charmantier, A., Cole, E. F., Eeva, T.,
677 Matthysen, E., Nater, C. R., Sheldon, B. C., Sæther, B.-E., Vriend, S. J. G., Zajkova, Z.,
678 Adamík, P., Aplin, L. M., Angulo, E., Artemyev, A., Barba, E., Barišić, S., ... Visser, M. E.
679 (2021). Connecting the data landscape of long-term ecological studies: The SPI-Birds
680 data hub. *Journal of Animal Ecology*, 90(9), 2147–2160. [https://doi.org/10.1111/1365-](https://doi.org/10.1111/1365-2656.13388)
681 [2656.13388](https://doi.org/10.1111/1365-2656.13388)

682 de Jong, G. (1993). Covariances Between Traits Deriving From Successive Allocations of a
683 Resource. *Functional Ecology*, 7(1), 75–83. <https://doi.org/10.2307/2389869>

684 de Jong, G., & van Noordwijk, A. J. (1992). Acquisition and Allocation of Resources: Genetic (CO)
685 Variances, Selection, and Life Histories. *The American Naturalist*, 139(4), 749–770.

686 de Villemereuil, P., Charmantier, A., Arlt, D., Bize, P., Brekke, P., Brouwer, L., Cockburn, A., Côté,
687 S. D., Dobson, F. S., Evans, S. R., Festa-Bianchet, M., Gamelon, M., Hamel, S., Hegelbach,
688 J., Jerstad, K., Kempnaers, B., Kruuk, L. E. B., Kumpula, J., Kvalnes, T., ... Chevin, L.-M.
689 (2020). Fluctuating optimum and temporally variable selection on breeding date in birds
690 and mammals. *Proceedings of the National Academy of Sciences*, 117(50), 31969–31978.
691 <https://doi.org/10.1073/pnas.2009003117>

692 Descamps, S., Gaillard, J.-M., Hamel, S., & Yoccoz, N. G. (2016). When relative allocation
693 depends on total resource acquisition: Implication for the analysis of trade-offs. *Journal*
694 *of Evolutionary Biology*, 29(9), 1860–1866. <https://doi.org/10.1111/jeb.12901>

695 Dingemanse, N. J., Araya-Ajoy, Y. G., & Westneat, D. F. (2021). Most published selection
696 gradients are underestimated: Why this is and how to fix it. *Evolution*, 75(4), 806–818.
697 <https://doi.org/10.1111/evo.14198>

698 Dingemanse, N. J., & Dochtermann, N. A. (2013). Quantifying individual variation in behaviour:
699 Mixed-effect modelling approaches. *Journal of Animal Ecology*, 82(1), 39–54.
700 <https://doi.org/10.1111/1365-2656.12013>

701 Dochtermann, N. A. (2011). Testing Cheverud’s Conjecture for Behavioral Correlations and
702 Behavioral Syndromes. *Evolution*, 65(6), 1814–1820. [https://doi.org/10.1111/j.1558-](https://doi.org/10.1111/j.1558-5646.2011.01264.x)
703 [5646.2011.01264.x](https://doi.org/10.1111/j.1558-5646.2011.01264.x)

704 Einum, S., & Fleming, I. A. (2000). Highly fecund mothers sacrifice offspring survival to maximize
705 fitness. *Nature*, 405(6786), 565–567. <https://doi.org/10.1038/35014600>

706 Fay, R., Authier, M., Hamel, S., Jenouvrier, S., van de Pol, M., Cam, E., Gaillard, J.-M., Yoccoz, N.
707 G., Acker, P., Allen, A., Aubry, L. M., Bonenfant, C., Caswell, H., Coste, C. F. D., Larue, B.,
708 Le Coeur, C., Gamelon, M., Macdonald, K. R., Moiron, M., ... Sæther, B.-E. (2022).
709 Quantifying fixed individual heterogeneity in demographic parameters: Performance of
710 correlated random effects for Bernoulli variables. *Methods in Ecology and Evolution*,
711 13(1), 91–104. <https://doi.org/10.1111/2041-210X.13728>

712 Fay, R., Hamel, S., van de Pol, M., Gaillard, J.-M., Yoccoz, N. G., Acker, P., Authier, M., Larue, B.,
713 Le Coeur, C., Macdonald, K. R., Nicol-Harper, A., Barbraud, C., Bonenfant, C., Van Vuren,
714 D. H., Cam, E., Delord, K., Gamelon, M., Moiron, M., Pelletier, F., ... Sæther, B.-E. (2022).
715 Temporal correlations among demographic parameters are ubiquitous but highly
716 variable across species. *Ecology Letters*, 25(7), 1640–1654.

717 <https://doi.org/10.1111/ele.14026>

718 Fay, R., Michler, S., Laesser, J., Jeanmonod, J., & Schaub, M. (2020). Can temporal covariation
719 and autocorrelation in demographic rates affect population dynamics in a raptor
720 species? *Ecology and Evolution*, *10*(4), 1959–1970. <https://doi.org/10.1002/ece3.6027>

721 Fischer, B., Taborsky, B., & Dieckmann, U. (2009). Unexpected Patterns of Plastic Energy
722 Allocation in Stochastic Environments. *The American Naturalist*, *173*(3), E108–E120.
723 <https://doi.org/10.1086/596536>

724 Fischer, B., Taborsky, B., & Kokko, H. (2011). How to balance the offspring quality–quantity
725 tradeoff when environmental cues are unreliable. *Oikos*, *120*(2), 258–270.
726 <https://doi.org/10.1111/j.1600-0706.2010.18642.x>

727 Fung, Y. L., Newman, K., King, R., & de Valpine, P. (2022). Building integral projection models
728 with nonindependent vital rates. *Ecology and Evolution*, *12*(3), e8682.
729 <https://doi.org/10.1002/ece3.8682>

730 Gabry, J., & Češnovar, R. (2020). *cmdstanr: R Interface to “CmdStan.”* [Computer software].

731 Gascoigne, S. J. L., Uwera Nalukwago, D. I., & Barbosa, F. (2022). Larval Density, Sex, and
732 Allocation Hierarchy Affect Life History Trait Covariances in a Bean Beetle. *The American*
733 *Naturalist*, *199*(2), 291–301. <https://doi.org/10.1086/717639>

734 Gebhardt, M. D., & Stearns, S. C. (1988). Reaction norms for developmental time and weight at
735 eclosion in *Drosophila mercatorum*. *Journal of Evolutionary Biology*, *1*(4), 335–354.
736 <https://doi.org/10.1046/j.1420-9101.1988.1040335.x>

737 Gelman, A., & Rubin, D. B. (1992). Inference from Iterative Simulation Using Multiple
738 Sequences. *Statistical Science*, *7*(4), 457–472. <https://doi.org/10.1214/ss/1177011136>

- 739 Gillespie, D. O. S., Russell, A. F., & Lummaa, V. (2008). When fecundity does not equal fitness:
740 Evidence of an offspring quantity versus quality trade-off in pre-industrial humans.
741 *Proceedings of the Royal Society B: Biological Sciences*, 275(1635), 713–722.
742 <https://doi.org/10.1098/rspb.2007.1000>
- 743 Hadfield, J. D. (2008). Estimating evolutionary parameters when viability selection is operating.
744 *Proceedings of the Royal Society B: Biological Sciences*, 275(1635), 723–734.
745 <https://doi.org/10.1098/rspb.2007.1013>
- 746 Hamel, S., Gaillard, J.-M., Douhard, M., Festa-Bianchet, M., Pelletier, F., & Yoccoz, N. G. (2018).
747 Quantifying individual heterogeneity and its influence on life-history trajectories:
748 Different methods for different questions and contexts. *Oikos*, 127(5), 687–704.
749 <https://doi.org/10.1111/oik.04725>
- 750 Healy, K., Ezard, T. H. G., Jones, O. R., Salguero-Gómez, R., & Buckley, Y. M. (2019). Animal life
751 history is shaped by the pace of life and the distribution of age-specific mortality and
752 reproduction. *Nature Ecology & Evolution*, 3(8), Article 8.
753 <https://doi.org/10.1038/s41559-019-0938-7>
- 754 Holtmann, B., Lagisz, M., & Nakagawa, S. (2017). Metabolic rates, and not hormone levels, are a
755 likely mediator of between-individual differences in behaviour: A meta-analysis.
756 *Functional Ecology*, 31(3), 685–696. <https://doi.org/10.1111/1365-2435.12779>
- 757 Kain, M. P., Bolker, B. M., & McCoy, M. W. (2015). A practical guide and power analysis for
758 GLMMs: Detecting among treatment variation in random effects. *PeerJ*, 3, e1226.
759 <https://doi.org/10.7717/peerj.1226>
- 760 Kendall, B. E., Fox, G. A., Fujiwara, M., & Nogeire, T. M. (2011). Demographic heterogeneity,

761 cohort selection, and population growth. *Ecology*, 92(10), 1985–1993.
762 <https://doi.org/10.1890/11-0079.1>

763 Kengeri, S. S., Maras, A. H., Suckow, C. L., Chiang, E. C., & Waters, D. J. (2013). Exceptional
764 longevity in female Rottweiler dogs is not encumbered by investment in reproduction.
765 *AGE*, 35(6), 2503–2513. <https://doi.org/10.1007/s11357-013-9529-8>

766 Knops, J. M. H., Koenig, W. D., & Carmen, W. J. (2007). Negative correlation does not imply a
767 tradeoff between growth and reproduction in California oaks. *Proceedings of the*
768 *National Academy of Sciences*, 104(43), 16982–16985.
769 <https://doi.org/10.1073/pnas.0704251104>

770 Krajick, K. (2004). All Downhill From Here? *Science*, 303(5664), 1600–1602.
771 <https://doi.org/10.1126/science.303.5664.1600>

772 Kroeger, S. B., Blumstein, D. T., Armitage, K. B., Reid, J. M., & Martin, J. G. A. (2020). Older
773 mothers produce more successful daughters. *Proceedings of the National Academy of*
774 *Sciences*, 117(9), 4809–4814. <https://doi.org/10.1073/pnas.1908551117>

775 Lack, D. (1947). The Significance of Clutch-size. *Ibis*, 89(2), 302–352.
776 <https://doi.org/10.1111/j.1474-919X.1947.tb04155.x>

777 Landes, J., Henry, P.-Y., Hardy, I., Perret, M., & Pavard, S. (2019). Female reproduction bears no
778 survival cost in captivity for gray mouse lemurs. *Ecology and Evolution*, 9(11), 6189–
779 6198. <https://doi.org/10.1002/ece3.5124>

780 Law, R. (1979). Optimal Life Histories Under Age-Specific Predation. *The American Naturalist*,
781 114(3), 399–417. <https://doi.org/10.1086/283488>

782 Link, W. A., & Eaton, M. J. (2012). On thinning of chains in MCMC. *Methods in Ecology and*

783 *Evolution*, 3(1), 112–115. <https://doi.org/10.1111/j.2041-210X.2011.00131.x>

784 Martin, J. S. (2023). *Covariance reaction norms: A flexible approach to estimating continuous*
785 *environmental effects on quantitative genetic and phenotypic (co)variances.*
786 <https://doi.org/10.32942/X2D89H>

787 McElreath, R. (2020). *Statistical Rethinking: A Bayesian Course with Examples in R and Stan* (2nd
788 ed.). Chapman and Hall/CRC. <https://doi.org/10.1201/9780429029608>

789 Melcher, J. C., Armitage, K. B., & Porter, W. P. (1990). Thermal Influences on the Activity and
790 Energetics of Yellow-Bellied Marmots (*Marmota flaviventris*). *Physiological Zoology*,
791 63(4), 803–820. <https://doi.org/10.1086/physzool.63.4.30158178>

792 Messina, F. J., & Fry, J. D. (2003). Environment-dependent reversal of a life history trade-off in
793 the seed beetle *Callosobruchus maculatus*. *Journal of Evolutionary Biology*, 16(3), 501–
794 509. <https://doi.org/10.1046/j.1420-9101.2003.00535.x>

795 Messina, F. J., & Slade, A. F. (1999). Expression of a life-history trade-off in a seed beetle
796 depends on environmental context. *Physiological Entomology*, 24(4), 358–363.
797 <https://doi.org/10.1046/j.1365-3032.1999.00151.x>

798 Metcalf, C. J. E. (2016). Invisible Trade-offs: Van Noordwijk and de Jong and Life-History
799 Evolution. *The American Naturalist*, 187(4), iii–v. <https://doi.org/10.1086/685487>

800 Milner, J. M., Elston, D. A., & Albon, S. D. (1999). Estimating the contributions of population
801 density and climatic fluctuations to interannual variation in survival of Soay sheep.
802 *Journal of Animal Ecology*, 68(6), 1235–1247. <https://doi.org/10.1046/j.1365->
803 2656.1999.00366.x

804 Mitchell, D. J., & Houslay, T. M. (2021). Context-dependent trait covariances: How plasticity

805 shapes behavioral syndromes. *Behavioral Ecology*, 32(1), 25–29.

806 <https://doi.org/10.1093/beheco/araa115>

807 Ozgul, A., Childs, D. Z., Oli, M. K., Armitage, K. B., Blumstein, D. T., Olson, L. E., Tuljapurkar, S., &
808 Coulson, T. (2010). Coupled dynamics of body mass and population growth in response
809 to environmental change. *Nature*, 466(7305), Article 7305.

810 <https://doi.org/10.1038/nature09210>

811 Paniw, M., Childs, D. Z., Armitage, K. B., Blumstein, D. T., Martin, J. G. A., Oli, M. K., & Ozgul, A.
812 (2020). Assessing seasonal demographic covariation to understand environmental-
813 change impacts on a hibernating mammal. *Ecology Letters*, 23(4), 588–597.

814 <https://doi.org/10.1111/ele.13459>

815 Pease, C. M., & Bull, J. J. (1988). A critique of methods for measuring life history trade-offs.
816 *Journal of Evolutionary Biology*, 1(4), 293–303. [https://doi.org/10.1046/j.1420-](https://doi.org/10.1046/j.1420-9101.1988.1040293.x)
817 [9101.1988.1040293.x](https://doi.org/10.1046/j.1420-9101.1988.1040293.x)

818 Péron, G., Gaillard, J.-M., Barbraud, C., Bonenfant, C., Charmantier, A., Choquet, R., Coulson, T.,
819 Grosbois, V., Loison, A., Marzolin, G., Owen-Smith, N., Pardo, D., Plard, F., Pradel, R.,
820 Toïgo, C., & Gimenez, O. (2016). Evidence of reduced individual heterogeneity in adult
821 survival of long-lived species. *Evolution*, 70(12), 2909–2914.

822 <https://doi.org/10.1111/evo.13098>

823 R Core Team. (2021). *R: A Language and Environment for Statistical Computing*. R Foundation
824 *for Statistical Computing*. [Computer software].

825 Réale, D., Reader, S. M., Sol, D., McDougall, P. T., & Dingemanse, N. J. (2007). Integrating animal
826 temperament within ecology and evolution. *Biological Reviews*, 82(2), 291–318.

827 <https://doi.org/10.1111/j.1469-185X.2007.00010.x>

828 Regan, C. E., Pemberton, J. M., Pilkington, J. G., & Smiseth, P. T. (2022). Having a better home
829 range does not reduce the cost of reproduction in Soay sheep. *Journal of Evolutionary*
830 *Biology*, 35(10), 1352–1362. <https://doi.org/10.1111/jeb.14083>

831 Reznick, D., Nunney, L., & Tessier, A. (2000). Big houses, big cars, superfleas and the costs of
832 reproduction. *Trends in Ecology & Evolution*, 15(10), 421–425.
833 [https://doi.org/10.1016/S0169-5347\(00\)01941-8](https://doi.org/10.1016/S0169-5347(00)01941-8)

834 Ricklefs, R. E., & Cadena, C. D. (2007). Lifespan is unrelated to investment in reproduction in
835 populations of mammals and birds in captivity. *Ecology Letters*, 10(10), 867–872.
836 <https://doi.org/10.1111/j.1461-0248.2007.01085.x>

837 Robinson, M. R., & Beckerman, A. P. (2013). Quantifying multivariate plasticity: Genetic
838 variation in resource acquisition drives plasticity in resource allocation to components of
839 life history. *Ecology Letters*, 16(3), 281–290. <https://doi.org/10.1111/ele.12047>

840 Roff, D. A. (1995). The estimation of genetic correlations from phenotypic correlations: A test of
841 Cheverud's conjecture. *Heredity*, 74(5), Article 5. <https://doi.org/10.1038/hdy.1995.68>

842 Salguero-Gómez, R., Jones, O. R., Jongejans, E., Blomberg, S. P., Hodgson, D. J., Mbeau-Ache, C.,
843 Zuidema, P. A., de Kroon, H., & Buckley, Y. M. (2016). Fast–slow continuum and
844 reproductive strategies structure plant life-history variation worldwide. *Proceedings of*
845 *the National Academy of Sciences*, 113(1), 230–235.
846 <https://doi.org/10.1073/pnas.1506215112>

847 Searle, S. R. (1961). Phenotypic, Genetic and Environmental Correlations. *Biometrics*, 17(3),
848 474–480. <https://doi.org/10.2307/2527838>

849 Sgrò, C. M., & Hoffmann, A. A. (2004). Genetic correlations, tradeoffs and environmental
850 variation. *Heredity*, 93(3), Article 3. <https://doi.org/10.1038/sj.hdy.6800532>

851 Simpson, E. H. (1951). The Interpretation of Interaction in Contingency Tables. *Journal of the*
852 *Royal Statistical Society: Series B (Methodological)*, 13(2), 238–241.
853 <https://doi.org/10.1111/j.2517-6161.1951.tb00088.x>

854 Skrondal, A., & Rabe-Hesketh, S. (2007). Redundant Overdispersion Parameters in Multilevel
855 Models for Categorical Responses. *Journal of Educational and Behavioral Statistics*,
856 32(4), 419–430. <https://doi.org/10.3102/1076998607302629>

857 Spigler, R. B., & Woodard, A. J. (2019). Context-dependency of resource allocation trade-offs
858 highlights constraints to the evolution of floral longevity in a monocarpic herb. *New*
859 *Phytologist*, 221(4), 2298–2307. <https://doi.org/10.1111/nph.15498>

860 Stearns. (1989). Trade-Offs in Life-History Evolution. *Functional Ecology*, 3(3), 259–268.
861 <https://doi.org/10.2307/2389364>

862 Stearns. (1992). *The Evolution of Life Histories*. Oxford University Press.

863 Stearns, de Jong, G., & Newman, B. (1991). The effects of phenotypic plasticity on genetic
864 correlations. *Trends in Ecology & Evolution*, 6(4), 122–126.
865 [https://doi.org/10.1016/0169-5347\(91\)90090-K](https://doi.org/10.1016/0169-5347(91)90090-K)

866 Stearns, S. C. (1984). The Effects of Size and Phylogeny on Patterns of Covariation in the Life
867 History Traits of Lizards and Snakes. *The American Naturalist*, 123(1), 56–72.
868 <https://doi.org/10.1086/284186>

869 Tavecchia, G., Coulson, T., Morgan, B. J. T., Pemberton, J. M., Pilkington, J. C., Gulland, F. M. D.,
870 & Clutton-Brock, T. H. (2005). Predictors of reproductive cost in female Soay sheep.

871 *Journal of Animal Ecology*, 74(2), 201–213. <https://doi.org/10.1111/j.1365->
872 2656.2005.00916.x

873 van Noordwijk, A. J., & de Jong, G. (1986). Acquisition and Allocation of Resources: Their
874 Influence on Variation in Life History Tactics. *The American Naturalist*, 128(1), 137–142.
875 <https://doi.org/10.1086/284547>

876 van Tienderen, P. H. (1995). Life Cycle Trade-Offs in Matrix Population Models. *Ecology*, 76(8),
877 2482–2489. <https://doi.org/10.2307/2265822>

878 Wells, C. P., Barbier, R., Nelson, S., Kanaziz, R., & Aubry, L. M. (2022). Life history consequences
879 of climate change in hibernating mammals: A review. *Ecography*, 2022(6), e06056.
880 <https://doi.org/10.1111/ecog.06056>

881 Williams, G. C. (1966). Natural Selection, the Costs of Reproduction, and a Refinement of Lack's
882 Principle. *The American Naturalist*, 100(916), 687–690. <https://doi.org/10.1086/282461>

883 Wilson, A. J., & Nussey, D. H. (2010). What is individual quality? An evolutionary perspective.
884 *Trends in Ecology & Evolution*, 25(4), 207–214.
885 <https://doi.org/10.1016/j.tree.2009.10.002>

886

887

888

889

890

891

892

893 **Supplementary materials**

894 **Section S1: fixed individual heterogeneity**

895 The models presented in the main text do not include distinct parameters for fixed individual
896 heterogeneity across environmental contexts, hence considering observations from the same
897 individual but in different environmental contexts as independent. Here, we illustrate why this
898 limitation is needed to correctly estimate context-dependent covariation. Using simulated data,
899 we illustrate that it is not possible to estimate the among-individual variation across context,
900 while at the same time estimating among- and within- individual variation within context.
901 However, it is important to note that not accounting for fixed individual heterogeneity should
902 not have any consequences regarding the accuracy of the estimation of the context-dependent
903 correlations.

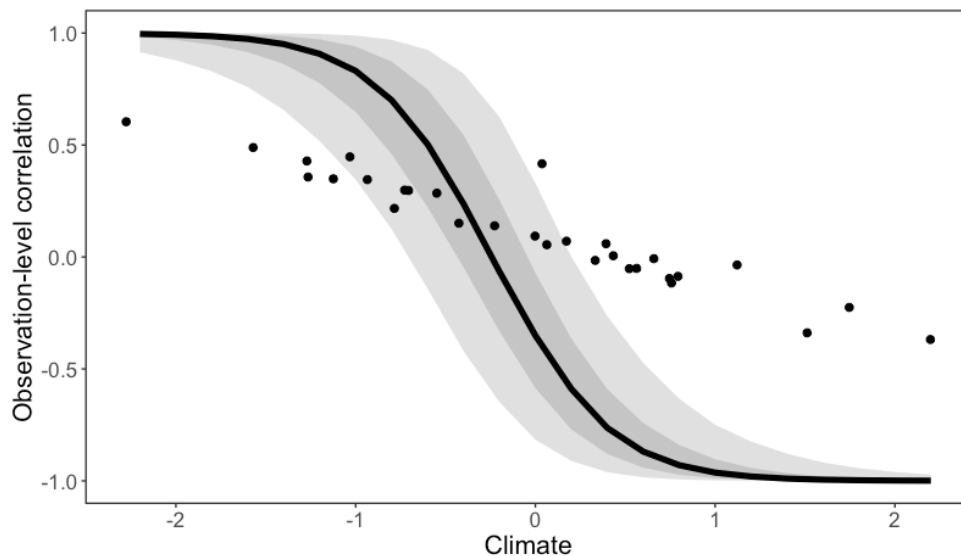
904 For this purpose, we simulate demographic data with a tradeoff between parental growth
905 and fecundity, suitable for the non-repeated measures CRN (model of equation 2). We include a
906 fixed heterogeneity component (context-independent individual random effect), as well as the
907 context-dependent component (context-dependent individual random effect) to make the
908 correlation vary across contexts. The data is similar to what is presented in the “validation on
909 simulated datasets” section, with the addition of the fixed heterogeneity component. We then
910 analyze this simulated dataset either with a model that estimates only the context-dependent
911 covariation (model presented in the manuscript, equation 2), or a model that does include fixed
912 (context-invariant) individual random effects in addition to the context-dependent covariation
913 (model of equation 2 with the addition of a context-independent individual random effect).

914 The figures for both scenarios are presented below, with Figure S1 highlighting that the
915 inclusion of a fixed among-individual random effect in the model leads to an erroneous
916 estimation of the context-dependent correlation. This is because the inclusion of this fixed
917 among-individual random effect captures part of the variation from the context-dependent
918 random effects, and therefore the context-dependent term will then only estimate deviations of
919 individuals from the fixed heterogeneity term. However, Figure S2 highlights that not including a
920 fixed among-individual random effect allows the model to properly recover the context-
921 dependent correlation.

922 Our results here reflect a more general theoretical point about the biological
923 interpretation of reaction norms. For any reaction norm model, there will not be a distinct
924 component of fixed individual heterogeneity separated from the process of phenotypic plasticity
925 shaping individual heterogeneity across environments. With simple linear reaction norms,
926 empiricists often conceptualize the intercept of the model as reflecting a fixed, environmentally
927 invariant component of the response, separate from the plastic effects described by reaction
928 norm slopes. However, while this can be heuristically useful for some purposes, it is in a strict
929 sense misleading, as the reaction norm intercept simply describes the variation expected when
930 the environmental variable defining the slope is fixed to 0 (e.g., in the average environment for
931 a mean-centered predictor or in the absence of an environmental exposure). Therefore, the value
932 of the intercept is no more fixed than the expected value at any other position along the slope
933 with respect to a fixed value of the environmental gradient. This thinking applies to the CRN and
934 any other reaction norm model. When sufficient data is available, individual random slopes could
935 also be estimated, which can be used to directly quantify the degree to which individuals' rank

936 order may shift across environments (Mitchell & Houslay, 2021). However, the depth of repeated
937 sampling required to fit such models for present purposes is unlikely to be achieved by many
938 currently existing datasets, motivating our CRN approach. Moreover, these random individual
939 slopes will generally be of less interest for detecting demographic tradeoffs, as compared to the
940 average shift in among-individual trait covariance across the population as determined by the
941 fixed CRN slopes.

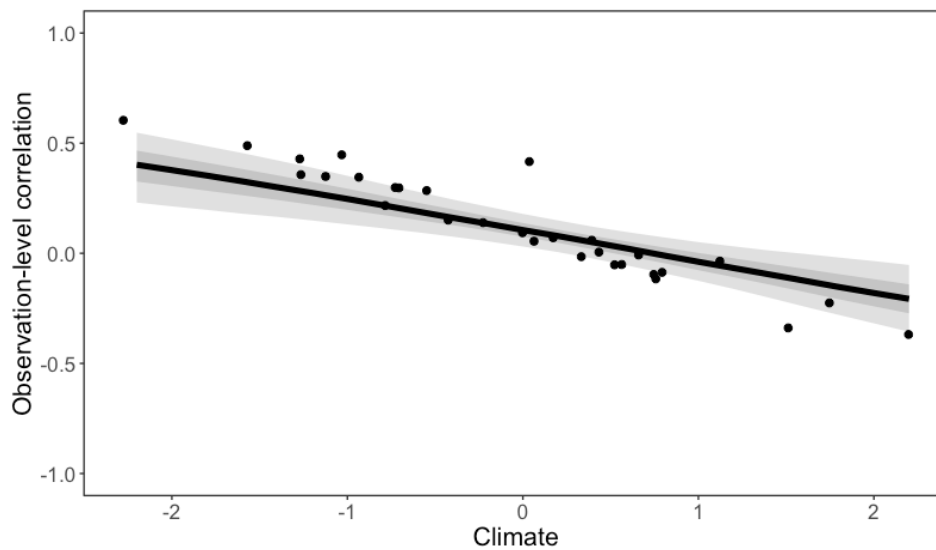
942 Taking a CRN approach to one's data thus requires taking seriously that there may not be
943 any biologically meaningful sense in which there is a fixed level of individual heterogeneity
944 irrespective of the environment (for traits that exhibit phenotypic plasticity). Rather, there is
945 simply the amount of individual heterogeneity given a particular environment, prior to exposure
946 to the environment, averaged across environments, and/or in the average environment. The
947 parameters from the CRN can always be used to predict any such quantities of interest. For
948 instance, applying the inverse link function to the intercept of the CRN (the first element of β_r)
949 will describe the expected trait correlation under the average environmental conditions.



950

951 Figure S1: Estimated context-dependent correlation when a fixed individual-random effect is
952 included. The regression line indicates the mean effect of climate on the correlation, while the
953 shaded areas depict the 50% and 89% credible intervals predicted by the model. Each black dot
954 represents the simulated observation-level correlation between both traits in a given year
955 depending on climate. This highlights that the inclusion of a fixed individual random effect leads
956 to a biased estimation of the context-dependent correlation.

957



958

959 Figure S2: Estimated context-dependent correlation without the inclusion of a fixed individual-
960 random effect in the model. The regression line indicates the mean effect of climate on the
961 correlation, while the shaded areas depict the 50% and 89% credible intervals predicted by the
962 model. Each black dot represents the simulated observation-level correlation between both traits
963 in a given year depending on climate. This highlights that not including a fixed individual random
964 effect leads to an appropriate estimation of the context-dependent correlation.

965

966

967

968

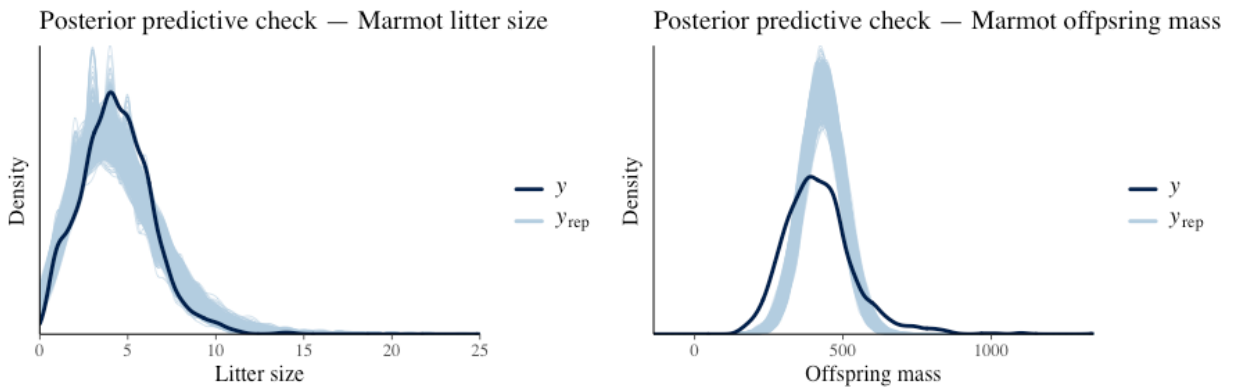
969

970

971

972

973 **Section S2: posterior predictive checks**



974

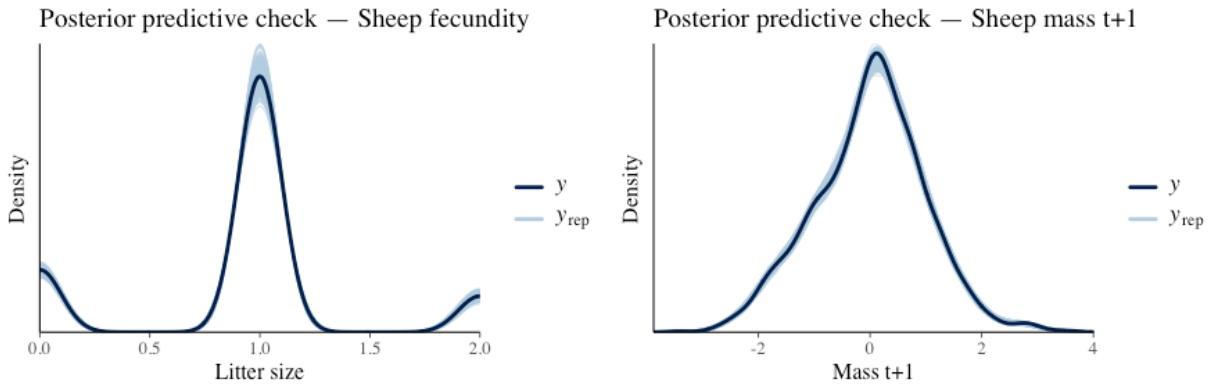
975 Figure S3: Posterior predictive checks showing the concordance between the distribution of the

976 data (y) and the distribution of data generated under the statistical model (y_{rep}), for litter size

977 (left panel) and offspring mass (right panel). This highlights a good fit for the litter size model. It

978 also highlights that there is a slight overdispersion in offspring mass that is not accounted for by

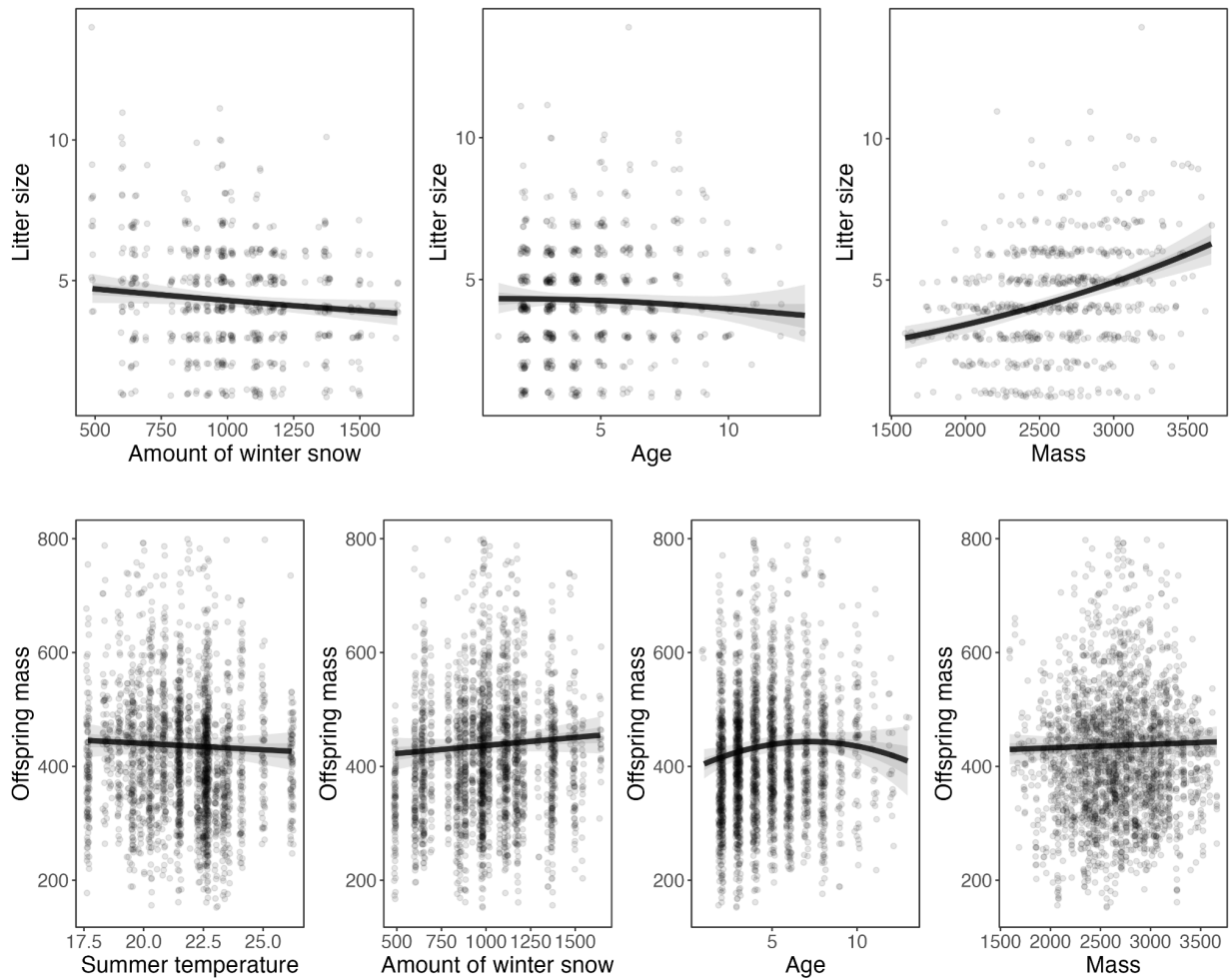
979 the model.



980

981 Figure S4: Posterior predictive checks showing the concordance between the distribution of the
 982 data (y) and the distribution of data generated under the statistical model (y_{rep}), for number of
 983 offspring (left panel) and ewe's mass in the following summer (right panel). This highlights a good
 984 fit for both the litter size and mass models.

985 **Section S3: associations between the covariates and traits studied**



986

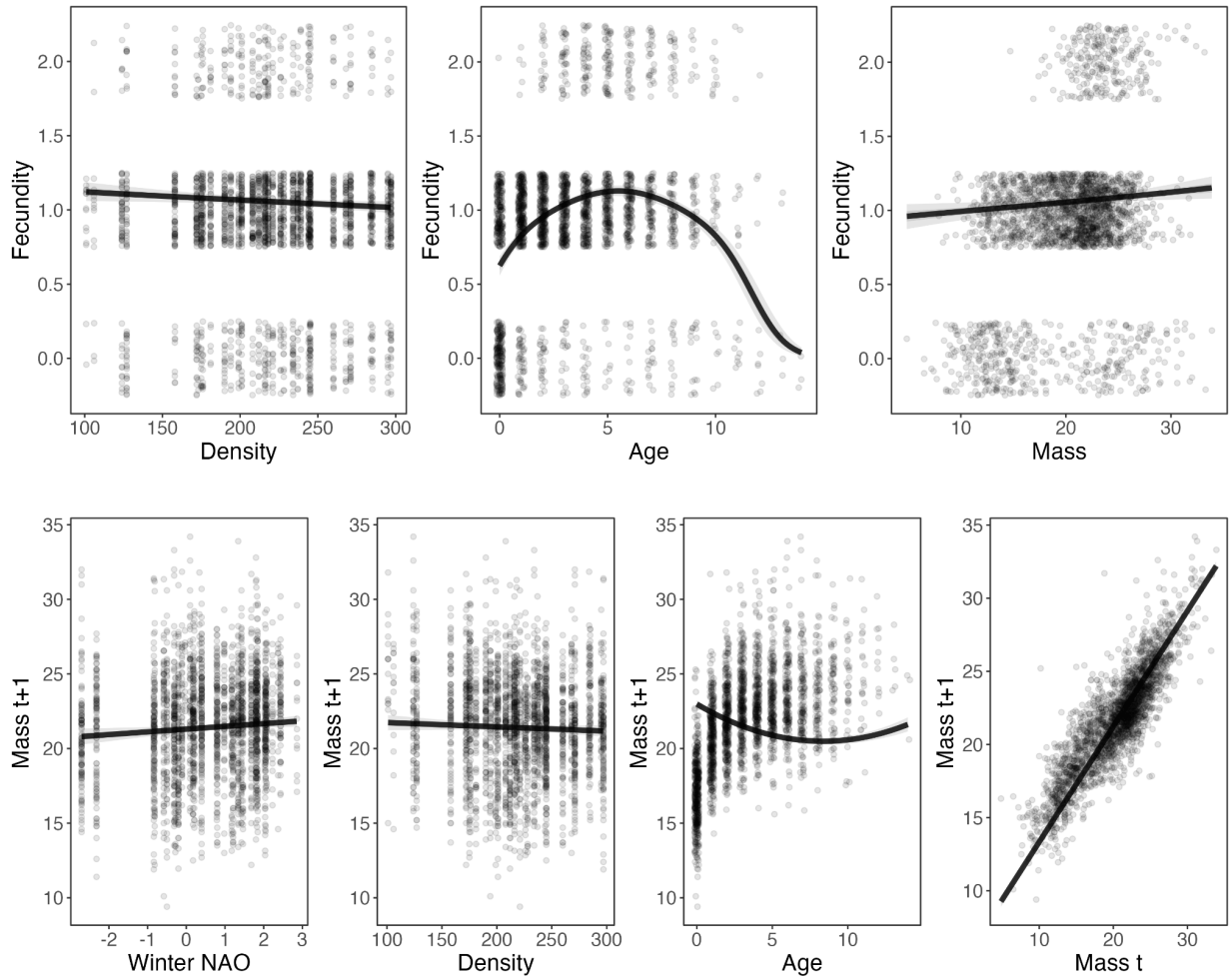
987 Figure S5: Top row: Association estimated by the model between the amount of winter snow,

988 age, and mass (panels from left to right) with litter size. Bottom row: Association estimated by

989 the model between summer temperature, the amount of winter snow, age, and mass (panels

990 from left to right) with offspring mass.

991



992

993 Figure S6: Top row: Association estimated by the model between population density, age, and

994 mass (panels from left to right) with fecundity. Bottom row: Association estimated by the model

995 between winter NAO, population density, age, and mass (panels from left to right) with mass at

996 t+1.